



HAL
open science

Structural and sedimentary origin of the Gargano - Pelagosa gateway and impact on sedimentary evolution during the Messinian Salinity Crisis

Romain Pellen, Daniel Aslanian, Marina Rabineau, Jean-Pierre Suc, William Cavazza, Speranta-Maria Popescu, Jean-Loup Rubino

► To cite this version:

Romain Pellen, Daniel Aslanian, Marina Rabineau, Jean-Pierre Suc, William Cavazza, et al.. Structural and sedimentary origin of the Gargano - Pelagosa gateway and impact on sedimentary evolution during the Messinian Salinity Crisis. *Earth Science Reviews*, 2022, 232, <10.1016/j.earscirev.2022.104114>. <insu-03846453>

HAL Id: insu-03846453

<https://insu.hal.science/insu-03846453v1>

Submitted on 25 Jul 2025

HAL is a multi-disciplinary open access archive for the deposit and dissemination of scientific research documents, whether they are published or not. The documents may come from teaching and research institutions in France or abroad, or from public or private research centers.

L'archive ouverte pluridisciplinaire HAL, est destinée au dépôt et à la diffusion de documents scientifiques de niveau recherche, publiés ou non, émanant des établissements d'enseignement et de recherche français ou étrangers, des laboratoires publics ou privés.



Distributed under a Creative Commons CC BY 4.0 - Attribution - International License

Structural and Sedimentary Origin of the Gargano - Pelagosa Gateway and Impact on Sedimentary Evolution during the Messinian Salinity Crisis

Romain Pellen¹, Daniel Aslanian², Marina Rabineau¹, Jean-Pierre Suc³, William Cavazza⁴, Speranta-Maria Popescu⁵, Jean-Loup Rubino³.

¹ Laboratoire Geo-Océan, Institut Universitaire Européen de la Mer, UMR6538, Rue Dumont d'Urville, 29280 Plouzané, France.

² IFREMER, Laboratoire Geo-Océan - Géodynamique et Enregistrement Sédimentaire, 1 place Nicolas Copernic, 29280 Plouzané, France

³ Institut des Sciences de la Terre Paris (ISTEP), UMR 7193, Laboratoire Evolution et Modélisation des Bassins Sédimentaires, Université P. et M. Curie - Paris 6, 75005 Paris, France

⁴ Department of Biological, Geological, and Environmental Sciences; Piazza di Porta S. Donato 1, 40100 Bologna, Italia

⁵ GeoBioStrataData consulting ; 385 Route du Mas Rillier, 69140 Rillieux la Pape, France.

Abstract

1 Circulation of water masses, sediment, and biotope between the sub-basins of the
2 Mediterranean Sea strongly depends on morphological oceanic gateways. These geological
3 features react to geodynamic reorganisation through volcanism, vertical movements, and/or the
4 segmentation of sedimentary basins. Despite the palaeogeographic relevance of straits and
5 oceanic-gateways, their evolution and impact on sedimentary transports and deposition in the
6 Mediterranean remain in general poorly constrained. The Gargano-Pelagosa gateway is here first
7 recognized as an influential element of the palaeogeographic/environmental evolution of the
8 central-southern Apenninic foredeep and wedge-top domains during the Messinian, as shown
9 by the integration of (i) seismic lines, (ii) well information from the Adriatic Sea, and (iii) a
10 review of both onshore and offshore structural data and Messinian depositional environments.
11 A palinspastic evolution is proposed for the Apennine and south Adriatic foredeeps during the
12 Messinian Salinity Crisis (MSC: 5.97-5.33 Ma). We highlight the implication of the pre-MSC
13 structural legacy and the development of the Apennine and Dinarid-Albanian chains in 1) the
14 isolation of the Apennine foredeep from the deep central Mediterranean domains at the peak
15 of the MSC; 2) the vertical movements at the Gargano-Pelagosa structure and the Apulian
16 Platform and 3) their implication in the deposition of a chaotic sedimentary body.

Keywords: Mediterranean Sea, Segmented basin, Marine pathways, Messinian Salinity Crisis, Palaeogeographic and Palinspastic reconstruction.

Introduction

17

18 The paleocurrents, and therefore the evolution of the paleoclimate but also of the
19 dispersal of sediments and their deposition, is strongly linked to the presence and evolution of
20 straits which can act as open passages (oceanic gateways) or barriers (Straume *et al.*, 2020). In
21 the Mediterranean Sea, the present-day physiographic map shows a strong segmentation with
22 several major oceanic gateways (i.e. the Gibraltar, Sicilian, Aegean straits) and secondary oceanic
23 gateways (Figure 1). As circulation of water masses, sediment, and biotope between the sub-
24 basins of the Mediterranean Sea strongly depends on these morphological oceanic-gateways,
25 their evolution is of primary importance to understand the morphological and sedimentary
26 evolution of the different basins (e.g. Leever *et al.*, 2010; Flecker *et al.*, 2015; Palcu *et al.*, 2017;
27 Suc *et al.*, 2015; Balázs *et al.*, 2017, Pellen *et al.*, 2017; Amadori *et al.*, 2018; Camerlenghi *et al.*,
28 2020). This is particularly critical in the case of large relative sea-level variations, such as during
29 the MSC (5.97–5.33Ma) (Manzi *et al.*, 2013) when huge amount of gypsum was only deposited
30 along the Apennine Foreland (Manzi *et al.*, 2020), and a understanding approach of the
31 Mediterranean Sea needs very detailed local studies, such as for the Betic, Rifain, Balkan or
32 Iron Gate gateways (Figure 1; Betzler *et al.*, 2006; Krijgsman *et al.*, 2006; Suc *et al.*, 2011, 2015;
33 Do Couto *et al.*, 2016).

34

35 The Gargano-Pelagosa gateway, located on the Adria plate and separating the central and
36 the south Adriatic basins, perfectly displays the relationship between the inherited sedimentary
37 structure (e.g. Argnani, 2013), vertical tectonic motion and sea-level variation, and their impacts
38 on water mass exchange during the Neogene. To understand the relationship between each
39 process, we focus on the connection between the Adriatic foredeep, the South Adriatic Basin
40 (SAB) and the deep Ionian Sea (through the former Lagonegro Basin) during the Messinian
41 Salinity Crisis (MSC: 5.97-5.33 Ma) taking account of the pre-MSC inherited sedimentary
42 and/or tectonic features.

43 In this study, we describe the segmentation and tectonic history of each domain
44 surrounding the Gargano-Pelagosa gateway by compiling the onshore and offshore structural
45 and sedimentary features. These observations are completed by the compilation of borehole
46 data and seismic profiles between the Central Adriatic Basin (CAB) and the South Adriatic

47 Basin (SAB). This set of data allowed us to re-evaluate the relationships of MSC environment
48 history with the structural heritage and to present palinspastic and environmental
49 reconstructions for the Messinian period.

50 Regional setting

51 1. Early history of the Adria plate

52 The present-day structure of the central Mediterranean area and the Adria plate results
53 from the interaction between the African, European, Iberic and Adria plates since the breakup
54 of the mega-continent Pangea (for a review, see [Cavazza et al., 2004](#)).

55 Mesozoic palaeogeographic reconstructions suggest two main sub-orthogonal extensional
56 directions associated with the development of Neotethysian oceanic domains: NW-SE and NE-
57 SW ([Ciarapica and Passeri, 2002](#); in [Vezzani et al., 2010](#); [Stampfli and Hochard, 2009](#)).
58 Associated to these orientations several present-day NW-SE oriented carbonate platform and
59 basin systems have been identified ([Figure 2](#); [Zappaterra, 1994](#); [Wrigley et al., 2015](#); [Vezzani et](#)
60 [al., 2010](#)). The present-day situation and stratigraphic evolution of each platform and basin-
61 slope/deep-basin systems developed during Mesozoic and Cenozoic time is presented in [figures](#)
62 [2 and 3](#). Even if the nature, age and orientation of the Ionian Sea remain a subject of debate
63 (see [Dercourt, 1972](#); [Channell et al., 1980](#); [Mele, 2001](#); [Panza et al., 2003](#); [Vezzani et al., 2010](#);
64 [Roure et al., 2012](#); [Carminati et al., 2012](#); [Dellong et al., 2018](#); [van Hinsbergen et al., 2020](#)),
65 northward extension have been associated to this domain such as the south Adriatic Sea or the
66 deformed Mesozoic Sannio-Molise and Lagonegro basins.

67 2. A multi-segmented peri-Adriatic domain

68 The eastern border of the Adria plate is associated to the Dinarid and Albanid-Hellenid
69 fold-and-thrust belts ([Figure 2](#)). The Scutari-Pec lineament separates the two fold-and-thrust
70 belts and is interpreted as a major dextral polyphasic transform fault system ([Figure 2](#);
71 [Chorowicz et al., 1981](#); [Grubic and Marovic, 1991](#)) developed during Cretaceous and Cenozoic
72 time. The Dinarid chains was mainly formed during Eocene - Oligocene time and incorporates
73 large parts of the Adriatic-Dinaric platform systems (e.g. [Schmid et al., 2008](#); [Stampfli and](#)
74 [Hochard, 2009](#); [Korbar, 2009](#); [Handy et al., 2010](#); [van Hinsbergen et al., 2020](#)). The Albanid-
75 Hellenid chain underwent two supplementary tectonic and exhumation stages - from the
76 Middle-Late Miocene until the present-day ([Kilias et al., 2001](#); [Fraseri et al., 2009](#); [Pashko and](#)

77 [Aliaj, 2020](#)). During the Neogene, two subsidence phases are recorded leading to the formation
78 of the South Adriatic foredeep domain, the first in the Middle Miocene-Tortonian (Pannonian-
79 Tortonian stage), and the second in the Late Miocene-Pliocene (Pontian s.l.). The two phases
80 are separated by a short compressive phase at the Late Miocene ([Pashko and Aliaj, 2020](#)). At the
81 scale of the Albanid-Hellenide chain, the system would be affected by several phases of
82 counterclockwise rotations, and estimated at 40°ccw between 15-13 and 8 Ma and 10°ccw in
83 the Late Miocene-Pliocene ([van Hinsbergen et al., 2005](#); [Fraseri et al., 2009](#)).

84 On the western border the Apennine system is part of a wide peri-Mediterranean
85 orogenic system developed from late Oligocene to present, associated with the counter-
86 clockwise rotation of the Corsica-Sardinia blocks during the Early Miocene, and Tyrrhenian
87 Basin opening since Middle-Late Miocene (e.g. [Ricci Lucchi, 1986](#); [Boccaletti et al., 1990](#)).
88 [Figure 3](#) summarize the deformation stage associated to each Mesozoic palaeogeographic
89 domain now involved in the Central and South Apennine Chain, Several tectonic phases are
90 reported, each one implying the folding and imbrication of the cover succession detached
91 toward the foreland, and the progressive involvement of younger and easternmost fore-deep
92 basins ([Casero, 2004](#); [Ghielmi et al., 2010](#); [Vezzani et al., 2010](#); [Artoni, 2013](#)) ([Figures 2 and 3](#)).

93 *The Central Apennines* are delimited to the south by the Anzio-Ancona (A.A.) and Maiella-
94 Roccamonfina (M.R.) lineaments ([Figure 2](#)). The Central Apennine chain accreted the
95 Mesozoic Tuscany and Umbria-Marche pelagic domains ([Figures 2 and 3 - Vezzani et al., 2010](#);
96 [Fantoni and Franciosi, 2010](#)). Several Neogene tectonic phases are recorded along the
97 Apennine and are associated to the development of several foreland basins (see [Figure 3](#) and
98 [Ghielmi et al., 2010](#); [Vezzani et al., 2010](#) for further information), which were gradually
99 cannibalized by the Apennine chain.

100 *The Southern Apennine Chain* is delimited by the Anzio-Ancona lineament (A.A.) to the north
101 and the Calabria block to the south ([Figures 2](#)). The Neogene stratigraphy has been widely
102 studied (see [Vezzani et al., 2010](#); [Ascione et al., 2012](#); [Vitale and Ciarcia, 2013](#) for further
103 detail) and related palaeoenvironmental domains have been associated with the inherited
104 Mesozoic domains ([Vezzani et al., 2010](#); [Figure 3](#)). The first signs of Neogene deformation along
105 the Apennine platforms are dated to post-Burdigalian-Langhian ([Figure 3](#)). From late
106 Tortonian-early Messinian, the whole tectonic wedge, including the Apennine Platform,
107 overthrust the Sannio-Molise and Lagonegro basins ([Cippitelli, 2007](#); [Vitale and Ciarcia, 2013](#)).

108 This new tectonic phase implies the development of fore-deep successions along the Lagonegro
109 basin, until the late Messinian (Figure 3).

110 Since late Messinian several thrust fronts are activated along the south and central Apennine
111 fold-and-thrust belt led to the progressive incorporation of the Messinian foredeep (including
112 the Messinian Laga Basin) into the belt and marked the initiation of a late Messinian-early
113 Pliocene foredeeps (Figure 3; Milli *et al.*, 2007; Vezzani *et al.*, 2010; Artoni, 2013).

114 3. Structural features affecting the Gargano-Pelagosa gateway

115 Several structural features affect the Gargano Peninsula and Palagruža Island (Figure 2),
116 which mark the boundary between the south (SAB) and central (CAB) Adriatic basins. The
117 Gargano Peninsula is part of the Apulian foreland, the most uplifted portion of a wide NW-SE
118 trending flexural antiform influenced by both the SW-verging Dinaric-Hellenic and NE-verging
119 Southern Apennine orogens (Moretti and Royden, 1987; Argnani *et al.*, 1993; Hairabian *et al.*,
120 2015). Around the Gargano Peninsula at least three main structural features have been
121 described, but their relationship remains debated:

122 - **The Mid Adriatic Ridge (MAR)**, developed along a general NW-SE axis, at the interface
123 of the Apennine and Dinarid deformation fronts (Figure 2) (Finetti, 1982; Argnani and
124 Gamberi, 1995). It consists of an array of structural highs, 10-40 km wavelength anticlinal
125 structures and Triassic salt diapirism structures (Casero and Bigi, 2012). Sub-basins comprised
126 between salt structures observe Triassic to Miocene sedimentary layers and highlight the salt
127 diapir growth phase through time (Festa *et al.*, 2013).

128 - The SW-NE oriented **Tremiti Ridge** located north of the Apulian Platform and is
129 defined by Triassic salt diapirism (Figure 2). A Late Miocene deformation period have been
130 identified along this structural feature (e.g. Festa *et al.*, 2013), but not excluding earlier phases
131 during Cenozoic and Mesozoic. Sedimentary hiatus on top of the Tremiti ridge suggest repeated
132 emersion during Paleocene, Oligocene, and Messinian times (Andriani *et al.*, 2005).

133 - **The Mattinata Fault System (MFS)** is observed both on land and at sea (e.g. Argnani *et al.*
134 *et al.*, 2009; Billi *et al.*, 2007; Figure 2). The offshore Mesozoic and Tertiary succession defines a
135 series of E-W to NE-SW trending anticlines. Secondary anticlinal axes, oriented NW-SE, are
136 located south of the Mattinata system and connect further north to the main system. The
137 system extends onshore within the Gargano Peninsula promontory and delimits two former
138 Mesozoic shallow and deep environment domains by a NW-SE axis faulted system: the western

139 part is associated to Mesozoic carbonate platform deposit of the Apulian Platform and the
140 eastern part to slope-deep Mesozoic carbonate deposit. Several tectonic reactivations and strike-
141 slip motions linked to regional and tectonic phases are documented (Morelli, 2002; Argnani *et*
142 *al.*, 2009).

143
144 The relationship between the MAR, the Tremiti Ridge and the MFS remains uncertain,
145 as well as the importance of these features in a wider geodynamic framework or the possible
146 involvement of the Hercynian basement (Fantoni and Franciosi, 2008, 2010). These structures
147 have been interpreted as a micro-plate boundary linked to reorganisation of forces at the limits
148 of the Adria microplates (Scisciani and Calamita, 2009), or as an eastward verging fault system
149 delimiting the external Apennine deformation front (Bally *et al.*, 1986; Ori *et al.*, 1991; De
150 Alteriis, 1995; Scrocca, 2006; Casero and Bigi, 2012) and connected to the Apennine front
151 through the Tremiti Ridge (Funciello *et al.*, 1991; Festa *et al.*, 2013). Crustal thickness
152 modeling's suggest a thinner continental crust (~ 30 km) at the CAB-SAB transition (Ritzwoller
153 *et al.*, 2007), as well as a shallower Moho depth from the CAB to the SAB (Moho rise from 30
154 to 20 km; Riguzzi and Doglioni, 2020). No sharp discontinuities are highlighted by
155 tomographic modelling, but this does not invalidate the possibility of deep crustal structures or
156 geodynamic hinge line as observed by geophysical data in the Liguria-Provence or Valencia
157 basins (e.g. Afilhado *et al.*, 2015; Moulin *et al.*, 2015; Leroux *et al.*, 2015a, b; Pellen *et al.*, 2016).

158 The extension of the MAR towards the SAB is also problematic due to its possible
159 interaction with the Tremiti Ridge, and its proximity to the Gargano peninsula and the
160 Mattinata Fault System. In any case, these structures influence the vertical evolution of the
161 Gargano promontory and the marine corridor between CAB and SAB during tectonic
162 reorganisation phases (Festa *et al.*, 2013). These movements have been suggested during the
163 Cenozoic and Late Miocene (Scisciani and Calamita, 2009; Argnani *et al.*, 2009; Festa *et al.*,
164 2013), but have not been quantified. Argnani *et al.* (2009) suggested that the development of
165 the MSC succession west of the Mattinata fault system and the MAR could be assigned to a
166 change of motion along the MFS from sinistral to dextral strike-slip motion. While the
167 orientation and character of the different Mesozoic platform-basin domains primarily control
168 the CAB-SAB connections, the marine corridor is strongly influenced by these structures.
169 However many questions remain as to the origin of each structural features and role in the
170 isolation of the CAB.

171 Understanding the oceanic gateways evolution helps us to understand why different
172 sedimentary environments are observed on either side of the Gargano promontory during the
173 different stages of the Messinian crisis, such as the presence and absence of halite deposition in
174 the Caltanissetta and Po Plain basins respectively, although both basins presented similar water
175 depths (Amadori *et al.*, 2018; Camerlenghi *et al.*, 2020).

176 4. Present-day observation of the Messinian deposits across the Adria 177 plate

178 1. MSC evolution along the Adria plate

179 A consensus has been reached in the scientific community in subdividing the MSC into
180 three main stages at the Mediterranean scale (between 5.97 and 5.33 Ma), each of them well
181 time-constrained and characterized by specific evaporite deposits and palaeo-hydrological
182 conditions (Clauzon *et al.*, 1997; CIESM, 2008; Roveri *et al.*, 2014; Manzi *et al.*, 2013, 2020).
183 Nevertheless, in detail, this consensus is not so large considering the various options discussed
184 in CIESM (2008) but restricted to one option only in Roveri *et al.* (2014). This is also
185 demonstrated by recent investigations on deep Messinian basins using industry drilling results
186 and seismo-stratigraphy (e.g. CIESM, 2008; Gorini *et al.*, 2015; Roveri *et al.*, 2016; Madof *et al.*,
187 2019; Andretto *et al.*, 2021a,b), these three stages may not be applicable everywhere in deep
188 water basins (essentially the Eastern Mediterranean and Levant basins). Accordingly, we follow
189 the Bache *et al.* (2015)'s chronology which takes into account all the recent robust data:

- 190 – Stage 1 (5.97-5.60 Ma) is associated with the development of shallow-water primary
191 evaporites (present only in marginal basins) (Clauzon *et al.*, 1997; CIESM, 2008), while
192 organic-rich shales sedimented in deeper water (Manzi *et al.*, 2007). Up to 16 shale-gypsum
193 cycles were deposited in relation to strong astronomical control and restriction of marine
194 water connection between the Atlantic and Mediterranean domain through the Rifian and
195 Betic corridors (Krijgsman *et al.*, 1996; Hilgen *et al.*, 2007; Lugli *et al.*, 2010).
- 196 – Stage 2 (5.60-5.55 Ma) marks the MSC paroxysm defined by the drastic marine water
197 exchange restriction between the Atlantic and Mediterranean seas leading to an important
198 sea-level drop in a hypersaline deep-basin system, sedimentary transfer to the deeper marine
199 areas, and uplift and deep fluvial erosion along the marginal domains (Clauzon *et al.*,
200 1997). Estimates of sea-level drop magnitude at the Mediterranean scale range from 100-
201 200 m (Manzi *et al.*, 2018) to 650-900 m (Amadori *et al.*, 2018; Ben-Moshe *et al.*, 2020),

202 1000 m (Pellen *et al.*, 2019) or 1500 m (Clauzon *et al.*, 1997; Bache *et al.*, 2009; Lofi *et al.*,
203 2011), according to basin physiography and/or scenario hypotheses. The exact timing of
204 deposition between east and west Mediterranean sub-basins and the presence of shallow vs.
205 deep environments are still a matter of debate (Roveri *et al.*, 2014; Bache *et al.*, 2015;
206 Gorini *et al.*, 2015).

207 – Stage 3: the timing of the Mediterranean marine reflooding (comprised between 5.55 and
208 5.33 Ma) also remains intensely debated (Andreetto *et al.*, 2021a; Popescu *et al.*, 2021) with
209 a first numerical model proposing an ultra-rapid rise in sea level at the end of the
210 Messinian event (Garcia-Castellanos *et al.*, 2009, 2020) and models proposing a stepwise
211 reflooding of the Mediterranean domains based on seismic reflection data (Bache *et al.*,
212 2012, 2015; Gorini *et al.*, 2015). In this hypothesis, a late lowstand period (5.55 – 5.46 Ma)
213 is proposed to explain the rapid precipitation of halite in the deep settings (Bache *et al.*,
214 2015; Gorini *et al.*, 2015). This phase is associated with a relatively slow sea level rise,
215 which smoothed out the scarring of the MSC crisis producing a very flat marine
216 ravinement surface. At 5.46 Ma, the rapid sea level rise helped to preserve the scars of the
217 MSC crisis on the margin, later followed by a moderate sea-level rise at 5.33 Ma (Bache *et al.*
218 *et al.*, 2012; Popescu *et al.*, 2021). However, Bache *et al.* (2012) and Pellen *et al.* (2017)
219 showed that the Mediterranean marine waters re-entered later the Apennine foredeep, at
220 5.36 Ma.

221

222 **Figure 4** presents the present-day distribution of MSC-related deposits along the Adria plate
223 compiled from the literature. The identification and description of Messinian formations have
224 led to the subdivision of the Adria domain into three main subdomains: (1) the Central
225 Adriatic Basin (CAB) fringed by the north and central Apennine chains, limited to the south by
226 the Gargano Peninsula and Palagruža Island, (2) the south Apennine Chain bounded to the
227 east by the Apulian Platform, and (3) the South Adriatic Basin (SAB) bounded to the south by
228 the Otranto Strait and to the east by the outer Albanid front.

229 **ii. The central Apennine foredeep and the Central Adriatic Basin**

230 The Messinian stratigraphy of the CAB has been extensively studied with onshore and
231 offshore sedimentary observations (Selli, 1960; Roveri *et al.*, 1998, 2001, 2004, 2008a,b; Milli *et al.*
232 *et al.*, 2006, 2007; Popescu *et al.*, 2007, 2008; Lugli *et al.*, 2010), geophysical observations
233 (Ghielmi *et al.*, 2010, 2013; Rossi *et al.*, 2015), and land-sea correlations (e.g. Ori *et al.*, 1991;

234 [Artoni and Casero, 1997](#); [Roveri and Manzi, 2006](#); [Roveri et al., 2005, 2008](#); [Artoni, 2013](#);
235 [Pellen et al., 2017](#); [Manzi et al., 2020](#)). Significant effort has been made to simplify the
236 Messinian lithostratigraphy at a regional scale ([Roveri et al., 2008, 2014](#)) and to correlate
237 onshore with offshore deposits. [Table 1](#) summarizes the different studies and correlations of
238 Messinian formations across the Central Apennine belt ([Figure 4](#); [Table 1](#)). To simplify the
239 description of the Messinian lithostratigraphy of each area across the Adria plate in this study,
240 we adopted the nomenclature of [Roveri et al. \(2004, 2005\)](#).

241 The Messinian Apennine foredeep was formed by the migration of the Marnoso-arenacea
242 foredeep during the Late Tortonian-Early Messinian tectonic phase, and includes three main
243 depocenters along the CAB ([Figure 4](#)). Two megasequences ([Table 1](#) ; T_2 , MP, *sensu* [Roveri et](#)
244 [al., 2005](#)) have been associated with the Messinian Salinity Crisis and respectively dated
245 between ca. 8Ma - 5.6 Ma, and 5.6 - 5.33 Ma.

246 The upper section of the T_2 megasequence corresponds to the development in an active tectonic
247 setting of 1) the primary evaporites (Primary Lower Gypsum – PLG) from 5.97 Ma to 5.6 Ma
248 (stage 1) in marginal wedge-top basins and foreland domain (Vena del Gesso Fm., [Roveri et al.,](#)
249 [2003, 2005, 2006](#); [Rossi et al., 2015](#); [Manzi et al., 2020](#) - Gessoso Solifera Fm. (evaporate)) and
250 2) siliciclastic fan deltas which evolved laterally to anoxic clays and dolomicrites in the main
251 depocenters ([Milli et al., 2006, 2007](#); [Ghielmi et al., 2010, 2013](#)).

252 Associated with the MSC stage 2 and the reflooding step closing the crisis, the initiation of the
253 MP megasequence ([Table 1](#)) corresponds to a wide stratigraphic unconformity dated at 5.60 Ma
254 observed along the whole Apennine fold-and-thrust belt. This regional event is part of a major
255 change of depocenters and is called "intra-Messinian phase" ([Ciaranfi et al., 1973](#); [Elter et al.,](#)
256 [1975](#); [Di Nocera et al., 2006](#); [Colalongo et al., 1976](#); [Roveri et al., 2005](#); [Milli et al., 2007](#); [Bigi et](#)
257 [al., 2009, 2011](#); [Ghielmi et al., 2010](#); [Artoni, 2013](#)). The eroded products of marginal domains
258 were resedimented in deep basins (Resedimented Lower Gypsum – RLG, e.g. [Roveri et al.,](#)
259 [2001](#); [Artoni and Casero, 1997](#); [Artoni, 2003, 2013](#); [Roveri et al., 2014](#); [Milli et al., 2007](#)).
260 These formations generate the general structure of $p - ev_1$ Fm (post-evaporate Fm.), which
261 includes a regional scale rhyolitic cinerite dated at 5.532 +/-0.004Ma ([Cosentino et al., 2013](#)).
262 The $p - ev_1$ Fm. is devoid of fossils and mainly comprises thin-bedded siliciclastic turbidites
263 considered to have been deposited in deep, freshwater conditions ([Roveri et al., 2001](#)).

264 The base of the $p - ev_2$ Fm. is age debated (5.36 Ma in [Popescu et al., 2007](#); [Bache et al., 2012](#);
265 [Pellen et al., 2017](#); 5.42 Ma in [Roveri et al., 2014](#); [Manzi et al., 2020](#)) and could mark a change
266 from a regressive to transgressive trend in the post-evaporitic succession ([Manzi et al., 2020](#)).
267 The $p - ev_2$ Fm. is considered to have mostly been deposited in hypohaline conditions
268 ([Popescu et al., 2007](#); [Pellen et al., 2017](#)) and known for its content in Paratethyan fossils (Lago
269 Mare biofacies; [Selli, 1973](#); [Colalongo et al., 1976](#); [Corradini and Biffi, 1988](#)). Based on the
270 study of microfossils, at least four marine incursions are associated with $p - ev_2$ Fm. ([Popescu
271 et al., 2007](#) ; [Pellen et al., 2017](#)), which probably later invaded the Po Basin ([Channell et al.,
272 1994](#) ; [Sprovieri et al., 2008](#) ; [Violanti et al., 2007, 2011](#)) due to the compartmentalization of
273 the Apennine foredeep ([Amadori et al., 2018](#)).

274 3. The east Apulian Platform and the south Apennine fold-and-thrust belt

275 Contrary to the Central Apennine Messinian foredeep, the MSC deposits identified
276 along the South Apennine chain are located in a wedge-top depositional zone ([Amore et al.,
277 1988](#); [Chiocchini et al., 2003](#); [Pescatore et al., 2008](#); [Matano et al., 2005, 2014](#); [Barone et al.,
278 2006, 2008](#); [Vezzani et al., 2010](#); [Ascione et al., 2012](#)) or along the Apulian foreland system
279 ([Pellen, 2016](#); [Petrullo et al., 2017](#); [Manzi et al., 2020](#)).

280 On the foreland domain close to the Apulian Platform, the pre-MSc late Miocene
281 succession presents several stratigraphic gaps during Paleocene, Oligocene, upper Langhian and
282 Tortonian times ([Vezzani et al., 2010](#); [Petrullo et al., 2017](#)). On the Apulian Platform, a syn- or
283 post-Messinian breccia deposit directly overlies the upper Cretaceous to Middle Miocene
284 carbonate formation ([Figure 3](#); [Pellen, 2016](#); [Manzi et al., 2020](#)). Towards the western side of
285 the Apulian foreland and below the allochthonous nappes, pre-evaporitic Messinian marls,
286 primary evaporites and post-evaporite successions are preserved ([Petrullo et al., 2017](#)).

287 The allochthonous domain of the South Apennine Chain observe preserved pre-MSc and
288 MSC formations on top of the former Sannio-Lagonegro Mesozoic basin ([Matano et al., 2007](#);
289 [Vezzani et al., 2010](#)). Development of the MSC successions seems to occur in a syn-tectonic
290 setting ([Matano et al., 2007, 2014](#)) with 1) organic-rich marls and diatomites and 2) PLG (stage
291 1 of the MSC), partially eroded and overlapped either by RLG or Pliocene conglomerate
292 deposits depending on the tectono-stratigraphic context of the outcrop ([Matano et al., 2007](#)).
293 The absence of MSC formation belonging to a deep environment and/or foredeep system
294 below the present-day south Apennine Chain ([Matano et al., 2005, 2014](#); [Matano, 2007](#); [Manzi](#)

295 *et al.*, 2020) may suggest: 1) a shallow depositional environment along the Apulian Platform
296 system with a cannibalized deep Lagonegro domain or 2) in the case of the presence of such
297 deposits below the south Apennine Chain, the possibility of a deeper Messinian depositional
298 setting towards the south of the Apulian Platform edge and Lagonegro domain.

299 The SAB is the least studied of the three areas. The SAB Messinian deposits seem
300 disconnected from those of the CAB and borehole information (Sparviero 001 borehole; *Manzi*
301 *et al.*, 2020) shows the initiation of resedimented gypsum formation located along the SAB. The
302 southward extension to the Ionian Sea through the Otronto Strait is still a matter of question
303 (Figure 4). According to the nomenclature of *Lofi et al.* (2018), these deposits are interpreted as
304 a detrital formation (Complex Unit - *Manzi et al.*, 2020; Upper Unit in *Lofi et al.*, 2011 of
305 unknown origin. Their mapping and the tectonic/sedimentary processes associated with
306 Messinian deposition in the SAB remain relatively unknown.

307 Data and methodology

308 To characterize the development of Cenozoic and MSC units along the Central Adriatic
309 Basin (CAB) and South Adriatic Basin (SAB), we merged seismic reflection profiles studied
310 during the academia-industry program GRI *Méditerranée* (Groupement Recherche-Industrie)
311 and vintage industrial profiles obtained from the VIDEPI website
312 (<https://www.videpi.com/videpi/videpi.asp>) and reprocessed. Figure 05 present the
313 distribution of the seismic lines used in this study and highlight the line drawings presented
314 figures 7 and 8 (Non-interpreted seismic lines are illustrated in [supplementary material 1 and](#)
315 [2](#)). B The regional distribution of these profiles allows us to re-evaluate the Neogene seismo-
316 stratigraphy (Some of the main Neogene seismic horizons based on Videpi seismic lines are
317 published in *Pellen et al.*, 2021) and compare the development of the different stratigraphic
318 unit identified along the CAB and SAB. Information on available boreholes obtained from the
319 VIDEPI website was also integrated in order to calibrate and correlate the identified
320 megasequences between the SAB and CAB. This set of data led us to re-evaluate the
321 relationships of MSC palaeoenvironments history with the structural and sedimentary heritage
322 and to present a set of palinspastic and palaeoenvironmental reconstruction maps for that
323 period. These palinspastic maps were built using Placa (*Matias et al.*, 2005) and Placa4D
324 (*Pelleau et al.*, 2015) free softwares ([https://wwz.ifremer.fr/gm_eng/Products-and-services/Free-](https://wwz.ifremer.fr/gm_eng/Products-and-services/Free-softwares)
325 [softwares](#)).

326 Boreholes and seismic lines are illustrated in [Figure 5](#), which combines the MSC
327 sedimentary formations described earlier along the CAB and South Apennine Chain, and the
328 new cartography of the MSC units detailed in this section. [Table 2](#) presents the stratigraphic
329 charts used in this study for (i) borehole correlation along the Adriatic Sea ([Figures 2, 6a and](#)
330 [6b](#)) and (ii) seismic stratigraphic interpretation across the CAB ([Figure 7](#)) and SAB ([Figure 8](#)).
331 Beyond the age of the stratigraphic units, their delimitations are based on the recognition of
332 angular unconformities and erosive discontinuities.

333 Results

334 1. Post-Mesozoic sedimentary evolution between the CAB and SAB from 335 borehole observation

336 i. Observed structural features

337 The Gargano Peninsula and Palagruža Island (see location in [Figure 2](#)) mark the
338 boundary between the south (SAB) and central (CAB) Adriatic basins. The depth of the top of
339 the Mesozoic series reached in boreholes varies markedly between 2400-2900m in the SAB and
340 1700-2000m in the CAB ([Figures 6a, and 6b](#)). The transition between the two basins is
341 influenced by several structural features of different wavelengths.

342 The Gargano Peninsula is the most elevated portion of the Apulian foreland and is
343 influenced 1) by a north-westward bending within the entire CAB ([Figure 7](#) - SONE03-06)
344 under the influence of the NE-verging Apennine orogeny and 2) to a south-eastward bending
345 within the SAB under the influence of the SW-verging Dinaric-Hellenic orogeny ([Figure 8](#) -
346 SONE 09) ([Moretti and Royden, 1987; Argnani et al., 1993; Hairabian et al., 2015](#)).

347 Offshore observations confirm an antiformal structural high delimited by the MFS and
348 the MAR ([Figure 7](#)-SONE07; [Figure 8](#) - SONE08-09) which mainly affected Mesozoic
349 formations. Towards the southeast, at the termination of the MFS and MAR, this structural
350 high disappears ([Figure 8](#) - SONE09). Deformation decreases on either side of these structures
351 with the general development of Miocene depocenter ([Figure 5; Figure 8](#) - NOSE02-04,
352 SONE09). Towards the north and respectively west and east the MFS and MAR features
353 surround the Gargano Peninsula ([Figures 2, 5](#)). The transition between the CAB and SAB
354 corresponds to a narrow Mesozoic slope-to-basin corridor -cropping out on the eastern part of
355 the Gargano Peninsula- and strongly deformed by the MAR Mesozoic to present-day
356 deformation that can be observed along several seismic lines ([Figure7](#) - SONE03-07; [Figure 8](#) -

357 NOSE05) and could be associated with the structural basement/Mesozoic dome and Triassic
358 salt diapirism.

359 A minimum of 2 s twt difference in depth is observed between the undeformed basin
360 domain and the structural crest (Figure 8 - SONE08 (km120)), suggesting >3 km uplift since
361 the Late Cretaceous and affecting the Gargano Peninsula. These deformation pulses may
362 correlate with the development of several sedimentary hiatuses (see next section). Together with
363 the development of the MAR, one of the main impacts could be the disconnection between the
364 CAB and SAB through the Gargano-Pelagosa corridor including during the MSC.

365 2. Post-Mesozoic to Miocene megasequences

366 Seven megasequences were defined from borehole correlation and seismic interpretation
367 (Figures 6a, 6b, 7, 8, 9). In this study we have focused our description on three megasequences:
368 the Paleocene-Eocene and Oligocene, Miocene pre-MSC, and Messinian syn-MSC
369 megasequences.

370 The **Paleogene-Eocene and Oligocene** megasequences mainly developed at the foot of the
371 slopes of ancient Mesozoic carbonate platforms (i.e. Fantoni and Franciosi, 2010) or along the
372 Dinarid fold-and-thrust belt in preserved foredeep depocenters (Figures 7, 8 - NOSE03,
373 SONE03-04-08). On the Apulian Platform, a sedimentary hiatus is observed at the top (Figure
374 6b, boreholes Sonia 001, Rovesti 001) and is locally associated with breccia deposits (Figure 6b,
375 borehole Edgar 002). Sediment are mainly composed limestone and argillaceous limestone
376 along the CAB. Important Paleogene-to-Oligocene depositional and/or erosional hiatuses are
377 locally observed on the Apulian Platform (Figure 6b - Sonia 001) or east of the Gargano
378 Peninsula on the uplifted part of the Mesozoic Ionian domain (Figure 6a - Cigno Mare).
379 Casero and Bigi (2012) also observed a Late Mesozoic-Burdigalian depositional hiatus north of
380 the Gargano Peninsula. Other boreholes from this area show older hiatuses from the Coniacian
381 to the Tortonian (Gargano Mare 001; Pellen, 2016). Within the SAB, a hiatus is observed at
382 the Late Cretaceous–Eocene interval (Figures 6a, 6b - Sparviero bis), followed by an important
383 deposition of carbonate and silt-marl during the Miocene.

384 The **Aquitanian to Messinian pre-MSC megasequence of the CAB and SAB** is mainly
385 developed along the SAB along the former basinal Mesozoic domain. It is divided into two sub-
386 sequences: Aquitanian-Langhian (Bisciario formation) and Serravallian-Tortonian (Schlier
387 formation). It is one of the series marking the greatest difference between the CAB and the

388 SAB. The Miocene sequence in the CAB is marked by a condensed set of clay carbonates
389 (average thickness of about 50 m) at the top of the carbonate platforms. Around the Gargano
390 Peninsula, carbonate formations are either associated with Langhian-Tortonian formation
391 (Figure 6a, Branzino borehole located on the Apulian Platform) or Aquitanian-Burdigalian
392 formation (Figure 6a, Cigno Mare). The associated sedimentary hiatuses could either be the
393 result of (i) uplift or subsidence linked to the development of new tectonic phases along the
394 deformation fronts and/or (ii) emersion of the area related to tectonic and relative low sea
395 level.. Conformable Aquitanian-Tortonian marls and carbonates with an average thickness of
396 150-200m exist at the foot of the slope of the Apulian Platform. Along the SAB, the
397 Aquitanian-Tortonian megasequence fills the Mesozoic Ionian domain with a 900-m-thick
398 depocenter (i.e. Sparviero bis, Figure 6a). In detail, the northern area of the MFS shows an
399 Aquitanian-Burdigalian depocenter with carbonate to silt lateral transition (Figure 6a), whereas
400 the southern area shows a Serravallian-Tortonian depocenter (Figure 6b). A Langhian to
401 Piacenzian hiatus and an erosive unconformity mark the area east of the Gargano Peninsula
402 (Figure 6a - Cigno Mare) and could indicate emersion during this time span.

403 3. Development of the Messinian syn-MSC megasequence

404 From the seismic and borehole observation, at least four seismic units were identified
405 offshore across the CAB and SAB (Table 2)

406 4. The Central Adriatic Basin

407 The CAB domain is associated to two thin seismic unit named M1 and M2. The M1
408 Unit can be defined by its seismic facies and its lithological composition, whereas the M2 Unit
409 unit was described from borehole sections only (Figure 6a).

410 The M1-M2 unit is defined coherently in the western side of the CAB by two continuous
411 seismic reflection of high amplitude and low frequency. The thickness of the unit is
412 homogeneous (0.1 s twt thick about 60 m thickness) and develops locally between the Triassic
413 salt anticlines composing the MAR along the CAB (0.2 s twt thick; Figure 7 - SONE03). This
414 facies was not observed on the eastern part of the CAB and east of the MAR, perhaps due to a
415 different depositional environment and/or to post-Messinian polygenic erosive and wave-cut
416 surfaces (Figure 7 - SONE03-04-06). From a lithological point of view (Figure 6a, 6b), M1
417 shows a basal clayey carbonate and marl formation (close to the Italian coastline) (Figure 6b -
418 Silvana 001). This succession is conformably covered by gypsiferous beds alternating with either

419 clay or carbonate levels and associated with the PLG (see [Manzi et al., 2020](#) for a review). In
420 some boreholes, the PLG are conformably covered by a 10-m-thick section of clayey carbonate
421 named in this study as the M2 Unit. Along the central part of the CAB, the Messinian units are
422 cut by an erosive surface ([Figures 6a, 6b, 7](#)), locally marked by a strong V-shaped incisions
423 ([Figure 7 - NOSE03](#)) suggesting a subaerial origin. At least three east-west oriented incised
424 valley systems were observed ([Figure 5](#)), but their origins as well as their terminations could not
425 be determined mainly due to the scarcity of seismic coverage in this study. According to our
426 observations, the M1 and M2 units do not appear connected with the other MSC deposits
427 identified along the SAB ([Figure 5; Figure 7 - SONE07; Manzi et al., 2020](#)).

428 5. The South Adriatic Basin

429 **The SAB domain** is characterized by two main MSC units ([Figure 5](#)) named M3 and M4,
430 and delimited by three erosional discontinuities S20, S22 and S30 ([Table 2](#)) which laterally
431 evolve into conformable surfaces toward the eastern part of the SAB ([Figure 8 - NOSE04-05](#)).
432 These units can be distinguished from the underlying formations by their seismic facies, their
433 internal geometries and the boundary surfaces.

434 Lithological observations are available for the Sparviero-bis borehole ([Figure 6a, 6b](#)),
435 which reaches the upper part of M3: In this area M3 lies on the Messinian Di Letto Fm.
436 (~100m) composed of sandy clay. The upper part of M3 may be associated with the Gessoso-
437 solfifera formation (about 70 m thick), here composed of alternating sandy-clay levels and
438 reworked evaporites. Gamma Ray and Sonic logs (Sparviero bis; Rovesti 001) suggest a detrital
439 origin for this formation instead of an in-situ evaporitic deposition as for the PLG ([this study;](#)
440 [Manzi et al., 2020](#)).

441 The base of M3 Unit is defined by an erosional surface of variable magnitude but traceable at
442 the scale of the entire SAB. The development of the M3 Unit is delineated south of the MFS,
443 on the northern edge of the Tremiti-MAR structure and is delimited south and north by the
444 platform edge of the Apulian and Adriatic platforms ([Figure 5](#)). The Mattinata and MAR
445 structures affect the morphology of the basal surface ([Figure 8, SONE09: km 20-70](#)), which
446 form a high relief compared to the SAB basin. M3 shows a different seismic facies between the
447 high MFS-MAR structure and the deeper domains, as well as lateral facies evolution towards the
448 southern SAB domain ([Figure 9](#)).

449 Southwest of the Mattinata system, M3 is characterized by poor-continuity reflections of
450 medium amplitude and medium frequency (Figure 8 - NOSE02: km 35-50; Supplementary
451 material 2; Figure 9). A fan geometry can be seen in secondary fault systems. This seismic facies
452 evolves laterally into a chaotic seismic facies with numerous diffraction hyperboles following a
453 SW-NE axis, interpreted as a clastic mass transport deposit (MTD) (Figure 5; Figure 8; Figure 9).
454 The detrital sediments, likely charged in gas, obscure the base of the unit and the underlying
455 formations. The development of the MTD facies limits monitoring of the basal erosional
456 unconformity, thus a maximum thickness of 0.6 s twt is proposed for M3 (Figure 8 - NOSE02).
457 Its thickness is variable and estimated towards the north at 0.3 s twt, which suggests derivation
458 from the Apulian Platform edge.

459 The unit shows gradual seismic facies change towards the SE with the development of more
460 continuous and sub-parallel reflections (Figure 8 - NOSE02-SONE10; Figure 9). It is worth
461 noting the presence of a pre-Messinian prograding facies developing at the same place as the
462 pre-MSC progradations (Figure 8, NOSE02: km 30-60). In the deep domain of the SAB (Figure
463 7, SONE07: km 65-120), the edges are also associated with the development of forced
464 regression prisms, with an average thickness of 0.2 s twt (Figure 8, SONE08: km 100-115;
465 SONE09: km130-150).

466 Along the northern part of the SAB, the top of M3 (S22) is a discontinuity truncating the
467 reflectors of M3, as well as the Aquitanian-Tortonian series where syn-MSC seismic units are
468 absent. The surface becomes concordant towards the SE and underlines the roof of M3.
469 Locally, V-shaped incised valley axes are observed (Figure 8, SONE08: km 123-135; Figure 8,
470 NOSE06: km 95-108), probably related to a NW-SE valley axis developing along the Mesozoic
471 carbonate platform. The origin of the incised valley observed along the CAB remains difficult
472 to define (Figure 5).

473 M4 Unit is underlain by the S22 discontinuity and is characterized by continuous
474 reflections towards the SE, of high amplitude and medium frequency. The unit also expands
475 towards the SE of the SAB, with more than 0.2 s twt thickness, and fills the depressions at the
476 top of the M3 detrital unit (Figure 8 - NOSE02: km60-168 - NOSE04: km 60-148). Note that
477 prograding reflections develop along a NE-SW axis, within the old incised valley (Figure 8 -
478 NOSE07: km 30-40; SONE09: km 105-120). Basinward, the seismic reflections of M4 become
479 parallel to M3, but we could not estimate the evolution of its thickness towards the Albanid

480 front and the Otranto Strait. Although, due to the lack of information from borehole data, we
481 are unable to provide a direct age for its deposition, M4 corresponds to the development of a
482 transgressive unit and could be correlated to the Upper Evaporites (DSDP 372: [Hsü et al., 1978](#);
483 [Lofi et al., 2011](#); [Roveri et al., 2014](#)) observed in the Western and Central Mediterranean
484 basins.

485 Discussion

486 1. Evolution of marine corridors across the Adria plate during the Messinian 487 (7.2 – 5.33 Ma)

488 The identification of the Gargano-Pelagosa strait and its impact on the distribution of
489 MSC deposits makes it possible to draw detailed palaeotectonic-paleoenvironmental
490 reconstructions of the study area of the Pelagosa Strait during Messinian times ([Figures 10-15](#)).
491 For each stage, two maps show the palinspatic reconstruction and palaeoenvironmental
492 information of the area. The kinematic motion of the Calabria block, the Adria plate, and the
493 north Apulian block relative to the Corsica-Sardinia blocks (used as the fixed reference) were
494 restored using Placa4D software ([Matias et al., 2005](#)). [Figures 10](#) to [15](#) illustrate the palinspatic
495 evolution of the study area at 7.2, 5.9, 5.5, 5.36 and 5.3 Ma. [Figure 10a](#) (7.2 Ma) corresponds to
496 the transition between rifting and drifting in the future central Tyrrhenian domain ([Lymer et](#)
497 [al., 2018](#)) which also marks a new compressive phase along the Apennine belt ([Vezzani et al.,](#)
498 [2010](#); [Ghielmi et al., 2010, 2013](#)).

499 Following [Carminati et al. \(2012\)](#) and [Argnani et al. \(2014\)](#), we rotated the Calabria-
500 Peloritani block east of Sardinia and the north Gargano micro-block; however, these authors
501 did not provide angles for the rotation. To be coherent with the geological and geophysical
502 intraplate information, we applied an angle of -8.7° ([Table 3](#)) for the Calabria-Peloritain block
503 for a total displacement of 450 km from 7.2 to 0Ma We also took into account a 10° ccw
504 rotation of the Albanid-Hellenide chain with a rotation point located at the Scutari-Pec
505 lineament ([van Hinsbergen et al., 2004](#)).

506 A second constraint comes from the restoration of the limit of the Adria plate and the
507 situation of the Mesozoic Adriatic, Apulia, and Apennine platforms. Palaeomagnetic data from
508 the Apennine Platform show a $\sim 60^\circ$ ccw rotation ([Gattacceca and Speranza, 2002](#)) and
509 constraints from thrust-top sedimentary basins overlying the Southern Apennine chain show

510 ~40ccw rotation in the late Miocene (van Hinsbergen *et al.*, 2020). We elected a ~45 ccw
511 rotation of the Apennine Platform with respect to the Apulian Platform (van Hinsbergen *et al.*
512 (2020) (Figure 10). As suggested by Vezzani *et al.* (2010) and Vitale and Ciarcia (2013), the
513 Apennine and Apulian platforms are connected by a slope domain (Figure 10). This restoration
514 implies a ~200 km wide Sannio-Molise-Lagonegro Mesozoic basin system at the junction with
515 the Ionian Sea. Argnani *et al.* (2009) also suggested that along the MFS compressional
516 deformation dominated since the late Miocene, contributing to create the topographic
517 elevation of the Gargano promontory. According to Tondi *et al.* (2005), dextral component of
518 motion is compatible with the present-day stress field that could be active since the last 200 kyr
519 at rates of 0.8+/- 0.1 mm/yr (0.8+/-0.1 km/Myr). According to these results and assuming
520 constant motion during the Pliocene, total displacement of the deep Mesozoic domain north
521 and south of the Mattinata fault system would not exceed 10 km from the late Messinian to
522 Present.

523 The palaeoenvironmental maps are based on these palinspastic constraints and the
524 information on the Messinian sedimentary deposits described in the previous sections.
525 Bathymetry ranges are proposed according to the sedimentary domain, (shelves: 0-200 m;
526 slopes: 200-2,000 m; basins and deep domain: 2,000-4,000 m). These values represent average
527 estimates, as does the exact position of the coastline within areas of low constraint due to poor
528 preservation of sedimentary deposits, such as the southern part of the future South Apennine
529 Chain or along the Otranto corridor.

530 1. Prior to the onset of the MSC (from 7.2 Ma to 5.9 Ma) (Figure 10-11)

531 During late Tortonian-early Messinian (Figure 10a) the whole Apennine platform and the
532 Molise-Lagonegro Basin were embodied in the Apennine deformation belt (Vezzani *et al.*, 2010;
533 Vitale and Ciarcia, 2013) (. Flysch deposition is recorded on the Apennine Platform (Anversa
534 flysch; Figure 3) and along its eastern border on the Sannio-Molise Basin (Agnone flysch)
535 (Figure 3; Vezzani *et al.*, 2010). Calcarenite deposition along the western border of the Apulian
536 Platform (Figure 3) marks the initiation of its deformation (Vezzani *et al.*, 2010). During this
537 period the Laga Basin developed northeast of the deformed Apennine Platform (Milli *et al.*,
538 2006, 2007) (Figure 10a) which is part of the Marnoso-arenacea-Bolognana flexural basin (e.g.
539 Roveri *et al.*, 2003; Milli *et al.*, 2006, 2007; Artoni, 2013). This end-Tortonian deformation
540 phase subdivides the Apennine foredeep into more confined basins with the Po, Romagna, and

541 Laga basins, and records the turbiditic sandstone and mudstone formation of Bagnolo Fm. and
542 Laga Fm. (Table 01; Artoni, 2003; Ghielmi *et al.*, 2010) on top of the Serravallian-Tortonian
543 foreland ramp. Associated with this tectonic phase, the inner part of the outer Marnoso-
544 arenacea foredeep is involved in the fold-and-thrust belt (Ricci Lucchi, 1986).

545 This deformation phase also impacted the SE border of the Adria plate during the Messinian to
546 present-day (Figures 10a-15a; Frasheri *et al.*, 2009; van Hinsbergen *et al.*, 2020), with the
547 reactivation and uplift of the Albanid fold-and-thrust belt (Frasheri *et al.*, 1996, 2009), south of
548 the Scutari-Pec lineament. Accordingly, this deformation involved the SE terminal part of the
549 Apulian Platform, thus implying bending towards the south of the eastern part of the Apulian
550 Platform. According to Argnani *et al.* (2009), these late Miocene tectonic phases are associated
551 with a change in tectonic style along the Mattinata fault system, from normal and left-lateral
552 strike-slip motion to compressive dextral strike-slip motion (Figures 10a, 11a).

553 Therefore, prior to the initiation of the MSC (Figure 10b), the Apulian Platform was an
554 island respectively bordered east and west by the Gargano-Pelagosa, Lagonegro and Otranto
555 straits. Both marine corridors delimitate the Messinian Apennine foredeep system from the
556 deeper environmental domains (Figure 10b; Pellen *et al.*, 2017; Manzi *et al.*, 2020). At that time,
557 the Gargano-Pelagosa Strait developed wackestone and argillaceous deposits (Schlier Fm.;
558 Famoso001 borehole) suggesting a shallow to medium water depth (Figure 10b). Several
559 sedimentary hiatuses and traces of erosion are associated with this corridor, suggesting that the
560 Gargano Strait was shallow throughout the Cenozoic era (Patacca *et al.*, 2008) with periods of
561 emersions. This palaeogeographic configuration could be linked to 1) the uplift of the Apulian
562 Platform during Mesozoic and Cenozoic times associated with the Mattinata, Tremiti, and
563 MAR systems, and 3) the uplift of the western part of the Adriatic Platform domain with the
564 influence of the Dinarid-Albanid chains.

565 During late Tortonian-early Messinian time, the western border of the Molise-Lagonegro Basin
566 was progressively affected by the eastward propagation of the Apennine fold-and-thrust belt and
567 foredeep development (Agnone Fm.). According to the tectono-stratigraphic compilation of
568 Ciarcia and Vitale (2013), from 7.2 Ma to 5.9 Ma, the Lagonegro-Molise domain was largely
569 incorporated in the allochthonous tectonic wedge (Figures 10b-11b). The Lagonegro-Molise
570 Strait is therefore interpreted as a shallow marine corridor during the MSC where the
571 depocenters are occurring in a wedge-top or foreland setting.

572 Lastly, the Otranto Strait width remains hypothetical and dependent on the Albanid thrust-front
573 propagation. For our reconstruction, we chose the Mesozoic palaeogeographic domain
574 observed along the Albanid fold-and-thrust belt (the Sazani Platform domain (location [Figure 3](#))
575 associated with the Apulian Platform and the Ionian domain associated with the SAB). In this
576 reconstruction ([Figure 10b](#)), the Otranto Strait brings the SAB and the Ionian Sea into contact.
577 It is locked to the west by the Apulian Platform and to the east by the Albanid-Hellenide fold-
578 and-thrust belt. The Messinian to Pliocene tectonic phases affecting this chain may have
579 progressively limited the sedimentary transfer from the SAB toward the Ionian Sea.

580 2. First stage of the MSC (from 5.97 Ma to 5.6 Ma) ([Figures 11-12](#))

581 The onset of the Messinian Salinity Crisis with a drastic reduction in the marine
582 connection between the Mediterranean Sea and the Atlantic Ocean at 5.97 Ma ([Manzi et al.,](#)
583 [2013](#)). At this time, the Apenninic foreland was a shallow evaporitic marine domain (PLG Fm.;
584 [Lugli et al., 2010](#); [Manzi et al., 2020](#)) with an average palaeo-water depth not exceeding 200 m
585 ([Figure 11b](#)). It then evolves towards the deeper part into organic-rich barren shale ([Manzi et al.,](#)
586 [2007](#)). The Laga and Romagna basins formed the main foredeep depocenter with at least 2.5-
587 km-thick turbiditic deposition between 7.2 and 5.6 Ma ([Milli et al., 2007](#)), associated with
588 sediment sources related to the Apennine Chain and the Alps following a N-S palaeocurrent
589 and NW-SE paleocurrent direction ([Milli et al., 2007](#)). This depocenter was limited to the south
590 by 1) the uplift of the former Apennine domain, now embedded in the allochthonous tectonic
591 wedge, 2) the uplift of the Gargano-Pelagosa Strait, and 3) possible tectonic inversion along the
592 MAR and MFS ([Figure 11a](#)). This substantial uplift of the area could be related to the opposing
593 compressive reactivation of the Albanid and Apennine Chains ([Fantoni and Franciosi, 2010](#))
594 and/or the inversion of the MFS ([Argnani et al., 2009](#)). This motion may have led to a
595 restriction of the Gargano-Pelagosa Strait during stage 1 ([Figures 11b, 12b](#)), and/or even to
596 outright marine closure between 5.97 and 5.6 Ma, as no PLG Fm. has been observed along the
597 strait.

598 Narrow marine corridors could have existed along the former Molise-Lagonegro Strait during
599 stage 1, bordered to the west and east by the Apennine front propagation and the Apulian
600 Platform. The presence of decameter-sized PLG blocks on present-day wedge-top basin outcrops
601 along the south Apennine Chain ([Figure 16](#); [Matano, 2007](#); [Matano et al., 2014](#); [Manzi et al.,](#)
602 [2020](#)) confirms the deposition of shallow evaporitic formations along the deformation front
603 and/or on the Apulian foreland area. Along the Apennine foredeep, evaporitic deposits of this

604 period are interbedded with marine clays, indicating marine incursions into the shallow basins
605 and reconnection of the Mediterranean, as mainly evidenced by fish remains (Sturani, 1973;
606 Fontes *et al.*, 1987; Carnevale *et al.*, 2008) and dinoflagellate cysts (Bertini, 2006).

607 3. Second MSC stage (from 5.6 Ma to 5.55 Ma) (Figures 12-13)

608 The major Mediterranean Sea level drawdown that characterized the paroxysmal step of
609 the MSC occurred at 5.6 Ma (Clauzon *et al.*, 1996, 1997; Bache *et al.*, 2012, 2015; Gorini *et al.*,
610 2015). This period also corresponds to a new deformation phase recorded throughout the
611 central Mediterranean area and particularly along the Apennine fold-and-thrust belt (Figure 3;
612 Vezzani *et al.*, 2010; Milli *et al.*, 2007; Roveri *et al.*, 2008). The activation of several thrust fronts
613 along the Apennine fold-and-thrust belt as well as on the southern border of the Laga Basin led
614 to incorporate the Messinian foredeep in the belt and initiated a late Messinian-early Pliocene
615 foredeep (Figure 3; Figures 12a-13a; Milli *et al.*, 2007; Vezzani *et al.*, 2010; Artoni, 2012).

616 Several observations attest to a total disconnection of the Apennine foredeep with respect to
617 the SAB or the Ionian Sea. The marginal domains and thrust-top basins are affected by a
618 subaerial erosional surface; the deeper domains and foredeeps are associated with the
619 development of gypsum-rich turbidites resulting from the erosion of the PLG. The occurrence
620 of an incised-valley system on the foreland part (Figure 13b) confirms a relative sea-level fall
621 comprised between 200 and 800 m, following the flexural back-stripping results modelled by
622 Amadori *et al.* (2018). This relative sea-level fall estimate differs depending of the studied area
623 (marginal basin connected or disconnected to the deeper basins; the hydrogeological and
624 climatic system), where higher estimates of relative sea-level fall have been inferred for the
625 western and eastern Mediterranean (~1000-1500 m) through stratigraphic observation and
626 backstripping modelling (Leroux *et al.*, 2017; Ben-Moshe *et al.*, 2020; Pellen *et al.*, 2019).
627 Freshwater, probably supplied in abundance by the surrounding uplands (Alps: Fauquette *et al.*,
628 2015a; Apennines: Fauquette *et al.*, 2015b), filled the Apennine foredeep and Po Basin where
629 relatively high water levels persisted during the lowered Mediterranean Sea level in subaqueous
630 brackish environments (Lago Mare biofacies; Gillet, 1968; Colalongo *et al.*, 1976; Bellagamba,
631 1978; Corselli and Grecchi, 1984; Esu and Taviani, 1989; Faranda *et al.*, 2007; Gliozzi *et al.*,
632 2007; Popescu *et al.*, 2007; Esu, 2007; Bache *et al.*, 2012; Pellen *et al.*, 2017) (Figure 13b).

633 At 5.6 Ma, the western side of the Apulian Platform edge was overthrust by the tectonic
634 prism of the southern Apennine Chain (Figures 12a, 13a; Barone *et al.*, 2006; Matano, 2007;

635 *Vezzani et al., 2010; Matano et al., 2014*). The southern Apennines experienced a strong
636 tectonic phase as attested by syn-tectonic thrusting during the deposition of RLG and after the
637 erosion of PLG (*Figure 16; Matano, 2007*). This mass transport complex includes pluri-
638 decameter PLG blocks which suggest a close source of erosion and resettlement in the nearby
639 narrow and shallow environment. Important wedge uplifts were recorded by apatite fission-
640 track data (cooling ages clustering around 5.5 Ma; *Corrado et al., 2005; Mazzoli et al., 2008;*
641 *Ascione et al., 2012*), which suggest important horizontal and vertical motions from late
642 Messinian to the present. Along the Apulian foreland, the RLG deposits are also specific to the
643 footwall of normal faults associated with the Mesozoic extensional phase along the Apulian
644 Platform (*Manzi et al., 2020*). Along the western side of the Apulian foreland, breccia, erosive
645 surface or conglomerate deposits are observed in boreholes, overlain by early Pliocene marls
646 (*Figure 5; Pellen, 2016; Manzi et al., 2020*). These different observations suggest a relative sea
647 level drop either linked to a sea level fall and/or a tectonic uplift. A different sedimentary
648 history is preserved along the present-day south Apennine chain compared to the CAB and
649 central Apennine chain. These different observations suggest a complete disconnection between
650 the Messinian Apenninic foredeep and the deep Ionian Sea during the MSC paroxysm across
651 the Molise-Lagonegro Strait or the Gargano-Pelagosa Strait.

652 Along the SAB, the MSC paroxysm is associated with the development of a mass transport
653 deposit, embedded in the M3 seismic unit. The latter includes resedimented clastic gypsum
654 (*Figure 6b - Sparviero bis borehole*), which indicates the erosion and re-sedimentation of
655 primary evaporites. A possible origin of this MTD could be associated with the eastern Apulian
656 Platform edge and is synchronous with the development of M3 detrital unit during the MSC
657 paroxysm. As there is no major MSC fluvial system located west of the Apulian platform, a
658 possible origin for the MTD could be linked to slope destabilization and submarine landslide.
659 Third MSC stage (from 5.55 Ma to 5.33 Ma) (*Figures 13-15*).

660 An age of 5.46 Ma has been proposed for the marine reflooding of the Mediterranean
661 (*Bache et al., 2012, 2015; Gorini et al., 2015; Popescu et al., 2021*). However, marine waters did
662 not immediately enter the Apennine foredeeps because the marine ingression in such domain,
663 corresponding to the boundary between the p-ev1 and p-ev2 formations (see *Table 1; Popescu et*
664 *al., 2007*), has been precisely dated at 5.36 Ma (*Bache et al., 2012*). From 5.36 Ma (*Figure 14b*),
665 marine waters overflowed the paleobarrier made by the Gargano-Pelagosa gateway and
666 penetrated the Apennine foredeep composed of brakish water from Paratethyan origin (the

667 third Lago Mare biofacies in Popescu *et al.*, 2015). At least four overflows of marinewaters have
668 been suggested (Pellen *et al.*, 2017), which possibly later flooded the Po Basin (Channell *et al.*,
669 1994; Sprovieri *et al.*, 2008; Violanti *et al.*, 2011). From a brakish environment, this process was
670 probably forced, first by the isostatic response of the palaeo-barrier linked to the Apennine
671 deformation phase and/or to the reflooding of the Mediterranean Basin, and then by the
672 continuous global sea-level rise after 5.33 Ma (Figure 15b; Gorini *et al.*, 2015).

673 Three Lago Mare events have been distinguished and documented in the Mediterranean
674 Basin by Do Couto *et al.* (2014) and Popescu *et al.* (2015) but Roveri *et al.* (2014) considered
675 only one Lago Mare event on the basis of the Apennine foredeep data where only the third
676 Lago Mare event occurred (Pellen *et al.*, 2017). In a recent synthesis on this biofacies, Andreetto
677 *et al.* (2021a) surprisingly followed the model of one Lago Mare event for the whole
678 Mediterranean Basin although they confirmed the marine context of Lago Mare 1 and 3
679 (Andreetto *et al.*, 2021b) consistently with Do Couto *et al.* (2014), Clauzon *et al.* (2015), and
680 Popescu *et al.* (2015).

681 After 5.3 Ma and the marine reflooding of the Bradanic and Apennine foredeeps, two more
682 tectonic phases were recorded along the Apennine fold-and-thrust belt (Figure 3): Early-Middle
683 Pliocene and Late Pliocene-Early Pleistocene (Vezzani *et al.*, 2010; Artoni, 2013; Ascione *et al.*,
684 2012; Vitale and Ciarcia, 2013). These tectonic phases led to the inclusion of the Laga Basin
685 and other Messinian foredeep systems in the fold-and-thrust belt. The total estimated
686 shortening along the central Apennine Chain is estimated between 13 km (L.S to A.A.
687 lineaments) and 32 km (A.A. to M.R. lineaments) (Artoni, 2013; see Figure 2 for the location
688 of lineaments), depending on the segment affected by the deformation. Along the Southern
689 Apennine, the Apennine allochthonous wedge continued to be thrust over the Apulian
690 Platform (Mazzoli *et al.*, 2008). Active thrusting migrated to the underlying platform during the
691 Pliocene, and was accompanied by a switch from thin-skinned thrusting to thick-skinned
692 inversion-dominated shortening (Mazzoli *et al.*, 2000; Butler and Mazzoli, 2006; Shiner *et al.*,
693 2004; Ascione *et al.*, 2012). From 5.3 Ma to the present, the migration of the allochthonous
694 tectonic wedge has been estimated between 50 and 60 km (Ascione *et al.*, 2012).

695

2. Intra-Messinian isostatic rebound and platform destabilization

696

697

698

699

700

Neogene horizontal and vertical motion changes should have affected the morphology of the Gargano-Pelagosa gateway as well as the SAB: the MAR and MFS seem to delimitate the SAB into two sub-basins following a NW-SE axis (Figure 8). The eastern part of the basin has thicker Paleogene-Miocene, Messinian, and Pliocene-Quaternary sedimentary successions compared to the western sub-basin.

701

702

703

704

705

The distribution of the different MSC-related formations around the Gargano-Pelagosa strait provides cogent constraints on the palaeoenvironmental and tectonic evolution along the Adria plate (Figures 5, 11-15). Moreover, the development of the MTD (M3 seismic unit) - originated from the Apulian platform edge - could be associated to several tectonic and/or eustatic processes affecting the area.

706

707

708

709

710

711

712

713

714

715

716

717

718

719

720

721

722

723

724

Similar MSC deposits have been recognized along the Mediterranean: the Valencia-Menorca basins (Maillard *et al.*, 2006; Comeselle and Urgeles, 2016; Pellen *et al.*, 2019), the Alboran Sea (del Olmo and Comas, 2008; del Olmo, 2011), the Malta Escarpment (Micallef *et al.*, 2018; Garcia-Castellanos *et al.*, 2020). MTDs have been associated with various processes (Canals *et al.*, 2004; Moscardelli and Wood, 2007) in the case of the Messinian event. Their origin is associated with seismotectonic activity and/or strong sea-level fluctuation and marine gas-hydrates release, isostatic rebound, and adaptation of river equilibrium profiles. In view of their stratigraphic position in the Alboran and Valencia basins, the emplacement of the MTDs was dated at around 5.60 Ma as a consequence of the sea-level fall and ensuing isostatic rebound of the continental shelves (del Olmo and Comas, 2008; Pellen *et al.*, 2019). The development of MTDs along the Maltese Escarpment was associated with the rapid sea-level rise at the end of the MSC (Garcia-Castellanos, 2009; Micallef *et al.*, 2018), but a tectonic origin linked to the destabilisation of the platform cannot be ruled out. Modelling of isostatic rebound only linked to the withdrawal of water masses around the Gargano-Pelagosa Strait suggests isostatic uplift values between 200 and 1000 m (DeCelles and Cavazza, 1995; Cavazza and DeCelles, 1998; Gargani *et al.*, 2010; Amadori *et al.*, 2018). This wide range is dependent on the palaeogeography and the nature of the associated basins and landforms (Govers *et al.*, 2009) as well as the tectonic setting, and reflects the important vertical movements affecting the Mediterranean marginal domains. More than 1.3 km were measured on the Gulf of Lion

725 margin for the MSC period and associated with water withdrawal and large sediment transfers
726 (Rabineau *et al.*, 2014).

727 Major tectonic re-organization are documented along the Adria plate during the MSC: (1)
728 the intra-Messinian tectonic phase impact the whole Apennine chain (see Discussion 1.3) and
729 Albanid chain (e.g. Pashko and Aliaj, 2020); (2) change from sinistral to dextral strike-slip
730 motion and folding along the MFS have been documented for the late Miocene (Argnani *et al.*,
731 2009). Together with the abrupt changes in sea level, these tectonic processes are perfect
732 candidates to explain the establishment of the MTD (M3 unit) in the SAB.

733 At a regional scale other major tectonic change (Giaconia *et al.*, 2018) and major
734 magmatic pulse (Sternai *et al.*, 2017) are observed. These Mediterranean tectonic/magmatic
735 pulses have been also linked to a more global plate kinematic reorganization affecting the earth
736 during Messinian time (Leroux *et al.*, 2018). These changes in horizontal motion also affect the
737 sub-marine morphology and kilometer scale uplift have been documented world-wide
738 (Rabineau *et al.*, 2014; Masters *et al.*, 2020). As highlighted by Booth-Rea *et al.* (2018) or
739 Masters *et al.* (2020), these uplift affecting the gateways favoured the faunal and floral migration
740 between continents. The episodic emergence of the Gargano-Pelagosa gateway during the MSC,
741 and more generally during the Mesozoic and Cenozoic, could also explain the faunal migration
742 between the different Mesozoic platforms of the former Greater Adria plate (Zarcone *et al.*,
743 2010; van Hinsbergen *et al.*, 2020).

744 Conclusions

745 The Gargano-Pelagosa gateway is here first recognized as an influential element of the
746 palaeogeographic/environmental evolution of the central-southern Apenninic foredeep and
747 wedge-top domains during the Messinian, as shown by the integration of (i) seismic lines, (ii)
748 well information from the Adriatic Sea, and (iii) a review of both onshore and offshore
749 structural data and Messinian depositional environments. Several processes concur to explain
750 the isolation of the Apennine foredeep during the MSC. Primarily, NW-SE oriented Mesozoic
751 platforms and basins systems controlled the Neogene sedimentary environments around the
752 Gargano-Pelagosa Strait. Messinian tectonic rejuvenation along the Apenninic and Albanid
753 fold-and-thrust belts, the Mid-Adriatic Ridge and Mattinata Fault System, led to the isolation of
754 the Apennine foredeep during the MSC paroxysm. We propose a coherent tectonic and
755 environmental evolution along the Adria plate during the MSC:

- 756 1 During MSC stage 1, the CAB evolved into a large evaporitic basin (Manzi *et al.*, 2020)
757 only connected to the deep Mediterranean basins east and west of the Apulian Platform
758 through the Gargano-Pelagosa and Lagonegro straits, respectively.
- 759 2 During the initiation of the stage 2, the combined effects of the MSC sea-level fall and
760 the ensuing intra-Messinian tectonic rejuvenation along the Apennine Chain led to the
761 closure of the Lagonegro Strait. We suggest that the widespread deposition of mass
762 transport deposits across the SAB is related to the isostatic rebound along the Apulian
763 Platform. Tectonic inversion of the Mattinata Fault System could also be associated with
764 intra-Messinian tectonics. These multiple tectonic processes led to the closure of the
765 Gargano-Pelagosa Strait and isolation of the Apennine foredeep, as suggested by Pellen
766 *et al.* (2017) and Manzi *et al.* (2020).

767

768 In the same way, the Otranto Strait could have been also influenced during the MSC by the
769 isostatic rebound related to sea-level fall and sedimentary transfer, and by tectonic
770 deformation along the Albanid-Peloponnese fold-and-thrust belt. Further seismic and
771 borehole investigation could highlight the sedimentary relationship between the SAB and
772 the Ionian Sea.

773

774

Acknowledgment

775 We acknowledge the “Visibilità dei dati afferenti all’ attività di esplorazione petrolifera in
776 Italia (VIDEPI)” for the public release of borehole and seismic data and their easy access. This
777 work was supported by Action Marge project, Labex MER and the ISblue Theme 2 project, co-
778 funded by a post-doctoral grant awarded to R. Pellen by IFREMER and UBO. We are also
779 grateful to Alison Chalm for English proofreading.

780

Conflict of interest

781 We confirm that we have no conflicts of interest related to this research, this work is
782 original to its form and has not been published elsewhere, nor is under consideration for
783 publication elsewhere.

784

- 786 Afilhado, A., Moulin, M., Aslanian, D., Schnürle, P., Klingelhoefer, F., Nouzé, H., Rabineau, M.,
787 Leroux, E., and Beslier, M.-O., 2015, Deep crustal structure across a young passive margin from
788 wide-angle and reflection seismic data (The SARDINIA Experiment) - II. Sardinia's margin:
789 Bulletin de la société géologique de France, v. 186, p. 331-351.
- 790 Amadori, C., Garcia-Castellanos, D., Toscani, G., Sternai, P., Fantoni, R., Ghielmi, M., and Di Giulio,
791 A., 2018, Restored topography of the Po Plain-Northern Adriatic region during the Messinian
792 base-level drop—Implications for the physiography and compartmentalization of the palaeo-
793 Mediterranean basin: Basin Research, p. 1-17.
- 794 Amore, O., Ciampo, G., Ruggiero, E., Santo, A., and Sgrasso, I., 1988, La successione miocenica del
795 Matese nord-occidentale: nuovi dati biostratigrafici e conseguenti ipotesi paleogeografiche:
796 Memorie della Società Geologica d'Italia, v. 41, p. 311-319.
- 797 Andreetto, F., Aloisi, G., Raad, F., Heida, H., Flecker, R., Agiadi, K., Lofi, J., BLondel, S., Bulian, F.,
798 Camerlenghi, A., Caruso, A., Ebner, R., Garcia-Castellanos, D., Gaullier, V., Guibourdenche,
799 L., Gvirtzman, Z., Hoyle, T.M., Meijer, P.T., Moneron, J., Sierro, F.J., Travan, G., Tzevahirtzian,
800 A., Vasiliev, I., and Krijgsman, W., 2021a, Freshening of the Mediterranean Salt Giant: contro-
801 versies and certainties around the terminal (Upper Gypsum and Lago-Mare) phases of the Mes-
802 sinian Salinity Crisis: Earth-Science Reviews, v. 216, 103577.
- 803 Andreetto, F., Matsubara, K., Beets, C.J., Fortuin, A.R., Flecker, R., and Krijgsman, W., 2021b. High
804 Mediterranean water-level during the Lago-Mare phase of the Messinian Salinity Crisis: insights
805 from the Sr isotope records of Spanish marginal basins (SE Spain). Palaeogeography, Palaeocli-
806 matology, Palaeoecology, v. 562, 110139.
- 807 Andriani, G.F., Walsh, N., and Pagliarulo, R., 2005, The influence of the geological setting on the mor-
808 phogenetic evolution of the Tremiti Archipelago (Apulia, Southeastern Italy): Natural Hazards
809 and Earth System Sciences, v. 5, p. 29-41.
- 810 Argnani, A., 2013, The influence of Mesozoic palaeogeography on the variations in structural style along
811 the front of the Albanid thrust-and-fold belt: Italian Journal of Geosciences, v. 132, p. 175-185.
- 812 Argnani, A., 2014, Mesozoic palaeogeography of Adria: Hints on the origin of the Skutari-Pec Line: In:
813 Beqiraj, A., Ionescu, C., Christofides, G., Uta, A., Beqiraj, Goga, E., Marku, S. (Eds.). Proceed-
814 ings of XX CBGA Congress of the Carpathian-Balkan Geological Association, Tirana (Albania).
815 Special session of the Buletini i Shkencave Gjeologjike, v. 1, p. 120
- 816 Argnani, A., Favali, P., Frugoni, F., Gasperini, M., Ligi, M., Marani, M., Mattiotti, G., and Mele, G.,
817 1993, Foreland deformational pattern in the Southern Adriatic Sea: Annales Geophysicae, v.
818 36, p. 229-247.
- 819 Argnani, A., and Gamberi, F., 1995, Stili strutturali al fronte della catena appenninica nell'Adriatico
820 centro-settentrionale: Studi Geologici Camerti Special volume, v. 1, p. 19-27.
- 821 Argnani, A., Rovere, M., and Bonazzi, C., 2009, Tectonics of the Mattinata fault, offshore south Gar-
822 gano (southern Adriatic Sea, Italy): Implications for active deformation and seismotectonics in
823 the foreland of the Southern Apennines: Geological Society of America Bulletin, v. 121, p.
824 1421-1440.
- 825 Artoni, A., 1993, Modello sedimentario e di flessurazione di un tratto del margine adriatico in un
826 settore dell' Appennino Centrale: Ph.D. thesis - Università di Parma, p. 301 p.
- 827 Artoni, A., and Casero, P., 1997, Sequential balancing of growth structures, the late tertiary example
828 from the central Apennine: Bulletin de la société géologique de France, v. 168, p. 35-49.
- 829 Artoni, A., 2013, The Pliocene-Pleistocene stratigraphic and tectonic evolution of the Central sector of
830 the Western Periadriatic Basin of Italy: Marine and Petroleum Geology, v. 42, p. 82-106.
- 831 Ascione, A., Ciarcia, S., Di Donato, V., Mazzoli, S., and Vitale, S., 2012, The Pliocene-Quaternary
832 wedge-top basins of southern Italy: an expression of propagating lateral slab tear beneath the
833 Apennines: Basin Research, v. 24, p. 456-474.

- 834 Bache, F., Olivet, J.-L., Gorini, C., Rabineau, M., Baztan, J., Aslanian, D., and Suc, J.-P., 2009, Messini-
835 an erosional and salinity crises: view from the provence basin (Gulf of Lions, Western Mediter-
836 ranean). : Earth and Planetary Science Letters, v. 286, p. 139-157.
- 837 Bache, F., Popescu S.M., Rabineau, M., Gorini, C., Suc, J.P., Clauzon G., Olivet J-L., Rubino J-L.,
838 Melinte-Dobrinescu M.C., Estrada F., Londeix L., Armijo R., Meyer B., Jolivet L., Jouannic G.,
839 Leroux E., Aslanian D., Baztan J., Dos Reis A.T., Mocochain L., Dumurdzanov N., Zagorchev I.,
840 Lesic V., Tomic D., Cagatay M.N., Brun J-P., Sokoutis D., Csato I., Ucakus G., and Cakir Z.,
841 2012, A two-step process for the reflooding of the Mediterranean after the Messinian Salinity
842 Crisis: Basin Research, v. 23, p. 1-29.
- 843 Bache, F., Gargani, J., Suc J.-P., Gorini, C., Rabineau, M., Popescu, S.M., Leroux, E., Do Couto, D.,
844 Jouannic, G., Rubino, J.-L., Olivet, J.-L., Clauzon, G., Dos Reis, A., and Aslanian, D., 2015,
845 Messinian evaporite deposition during sea level rise in the Gulf Of Lions (Western Mediterra-
846 nean): Marine and Petroleum Geology, v. 66, p. 262-277.
- 847 Balázs, A., Granjeon, D., Matenco, L., Sztanó, O., and Cloetingh, S., 2017, Tectonic and climatic con-
848 trols on asymmetric half-graben sedimentation: inferences from 3-D numerical modelling: Tec-
849 tonics, v. 36, p. 2123-2141.
- 850 Bally, A.W., Burbi, L., Cooper, C., and Ghelardoni, R., 1986, Balanced sections and seismic reflection
851 profiles across the Central Apennines: Memorie della Società Geologica Italiana, v. 35, p. 257-
852 310.
- 853 Barone, M., Critelli, S., Le Pera, E., Di nocera, S., Matano, F., and Torre, M., 2006, Stratigraphy and
854 Detrital Modes of Upper Messinian Post-evaporitic Sandstones of the Southern Apennines, Ita-
855 ly: Evidence of Foreland-Basin Evolution during the Messinian Mediterranean Salinity Crisis:
856 International Geology Review, v. 48, p. 702-724.
- 857 Barone, M., Dominici, R., Muto, F., and Critelli, S., 2008, Detrital modes in a late Miocene wedge-top
858 basin, northeastern Calabria, Italy: compositional record of wedgetop partitioning: Journal of
859 Sedimentary Research, v. 78, p. 693-711.
- 860 Ben-Moshe, L., Ben-Avraham, Z., Enzel, Y., and Schattner, U., 2020, Estimating drawdown magnitudes
861 of the Mediterranean Sea in the Levant basin during the Lago Mare stage of the Messinian Sa-
862 linity Crisis: Marine Geology, v. 427.
- 863 Bellagamba, M., 1978. Gli "strati a Congerie" di Capanne di Bronzo (Pesaro) del Messiniano terminale
864 e deduzioni paleoambientali. Acta Naturalia dell'Ateneo Parmense 14, 207-222.
- 865 Bertini, A., 2006, The Northern Apennines palynological record as a contribute for the reconstruction
866 of the Messinian palaeoenvironments: Sedimentary geology, v. 78, p. 115-121.
- 867 Betzler, C., Braga, J.C., Martin, J.M., Sanchez-Almazo, I.M., Lindhorst, S., 2006, Closure of a seaway:
868 stratigraphic record and facies (Guadix basin, Southern Spain): Int J Earth Sci.
- 869 Bigi G., Castellarin A., Coli M., Dal Piaz G.V., Sartori R., Scandone P. & Vai G.B., 1990. *Structural*
870 *Model of Italy scale 1:500.000, sheet 1-6.* C.N.R., Progetto Finalizzato Geodinamica, SELCA Fi-
871 renze.
- 872 Bigi, S., Milli, S., Corrado, S., Casero, P., Aldega, L., Botti, F., Moscatelli, M., Stanzione, O., Falcini, F.,
873 Marini, M., and Cannata, D., 2009, Stratigraphy, structural setting and burial history of the
874 Messinian Laga basin in the context of Apennine foreland basin system: Journal of Mediterra-
875 nean Earth Sciences, v. 1, p. 61-84.
- 876 Bigi, S., Casero, P., and Ciotoli, G., 2011, Seismic interpretation of the Laga basin; constraints on the
877 structural setting and kinematics of the Central Apennines: Journal of the Geological Society,,
878 v. 168, p. 1-11.
- 879 Billi, A., Gambini, R., Nicolai, C., and Storti, F., 2007, Neogene-Quaternary intraforeland transpression
880 along a Mesozoic platform-basin margin: The Gargano fault system, Adria, Italy: Geosphere, v.
881 3, p. 1-15.
- 882 Boccaletti, M., Ciaranfi, N., Cosentino, D., Deiana, G., Gelati, R., Lentini, F., Massari, F., Moratti, G.,
883 Pescatore, T., Ricci Lucchi, F., and Tortorici, L., 1990, Palinspastic restoration and
884 paleogeographic reconstruction of the Peri-Tyrrhenian area during the Neogene:
885 palaeogeography, Palaeoclimatology, Palaeoecology, v. 77, p. 41-50.

- 886 Booth-Rea, G., Ranero, C.R., and Grevemeyer, I., 2018, The Alboran volcanic-arc modulated the Mes-
887 sinian faunal exchange and salinity crisis: *Nature Scientific Reports*, v. 8, p. 13015.
- 888 Bosellini, A., 2002, Dinosaurs "re-write" the geodynamics of the eastern Mediterranean and the paleo-
889 geography of the Apulia Platform: *Earth-Science Reviews*, v. 59, p. 211-234.
- 890 Butler, R.W.H., Lickorish, W.H., Grasso, M., Pedley, H.M., and Ramberti, L., 1995, Tectonics and
891 sequence stratigraphy in Messinian basins, Sicily: Constraints on the initiation and termination
892 of the Mediterranean salinity crisis: *Geological Society of America*, v. 107, p. 425-439.
- 893 Butler, R.W.H., and Mazzoli, S., 2006, Styles of continental contraction: a review and introduction: In:
894 *Styles of Continental Contraction* (Ed. by S. Mazzoli and R.W.H. Butler), GSA Special Paper, v.
895 414, p. 1-10.
- 896 Butler, R.W.H., Maniscalco, R., and Pinter, P.R., 2019, Syn-kinematic sedimentary systems as con-
897 straints on the structural response of thrust belts: re-examining the structural style of the Ma-
898 ghrebian thrust belt of Eastern Sicily: *Italian Journal of Geosciences*, v. 138.
- 899 Comeselle, A.L., and Urgeles, R., 2016, Large scale margin collapse during Messinian early sea-level
900 drawdown: the SW Valencia trough, NW Mediterranean: *Basin research*, v. 29, p. 576-595.
- 901 Camerlenghi, A., Del Ben, A., Hübscher, C., Forlin, E., Geletti, R., Brancatelli, G., Micallef, A., Saule,
902 M., and Facchin, L., 2020, Seismic markers of the Messinian salinity crisis in the deep Ionian
903 Basin: *Basin Research*, v. 32, p. 716-738.
- 904 Canals, M., Casamor, J.L., Lastras, G., Monaco, A., Acosta, J., Berné, S., Loubrieu, B., Weaver, P.P.E.,
905 Grehan, A., and Dennielou, B., 2004, The Role of Canyons in Strata Formation: *Oceanogra-
906 phy*, v. 17, p. 81-91.
- 907 Carnevale, G., Caputo, D., Landini, W., 2008. A leerfish (Teleostei, Carangidae) from the Messinian
908 evaporite succession of the Vena del Gesso basin (Romagna, Apennines, Italy): palaeogeograph-
909 ical and palaeoecological implications. *Bollettino della Societa` Paleontologica Italiana* 47, 169-
910 176.
- 911 Casero, P., 2004, Structural setting of petroleum exploration plays in Italy: *Italian Geological Society*.
- 912 Casero, P., and Bigi, S., 2012, Structural setting of the Adriatic basin and the main related petroleum
913 exploration plays: *Marine and Petroleum Geology*.
- 914 Carminati, E., Lustrino, M., and Doglioni, C., 2012, Geodynamic evolution of the central and western
915 Mediterranean: Tectonics vs. igneous petrology constraints: *Tectonophysics*, v. 579, p. 173-192.
- 916 Cavazza, W., and DeCelles, P.G., 1998, Upper Messinian siliciclastic rocks in southeastern Calabria
917 (southern Italy): palaeotectonic and eustatic implications for the evolution of the central Medi-
918 terranean region: *Tectonophysics*, v. 298, p. 223-241.
- 919 Cavazza, W., Roure, F., Spakman, Stampfli, G.M., and Ziegler, P.A., eds., 2004, *The TRANSMED At-
920 las: the Mediterranean Region from Crust to Mantle*: Heidelberg, Springer-Verlag, 141 pp. +
921 CD-ROM.
- 922 Centamore, E., and Nisio, S., 2003, Significant events in the Periadriatic foredeeps evolution (Abruzzo-
923 Italy). *Studi Geologici Camerti*, v. num. spec. 2003, p. 39-48.
- 924 Channell, J.E.T., Catalano, R., and D'Argenio, B., 1980, Paleomagnetism and deformation of the
925 Mesozoic continental margin in Sicily: *Tectonophysics*, v. 61, p. 391-407.
- 926 Channell, J.E.T., Poli, M.S., Rio, D., Sprovieri, R., and Villa, G., 1994, Magnetic stratigraphy and bio-
927 stratigraphy of Pliocene "argille azzurre" (Northern Apennines, Italy): *Palaeogeography, Palaeo-
928 climatology, Palaeoecology*, v. 110, p. 83-102.
- 929 Ciaranfi, N., Dazzaro, L., Pieri, P., Rapisardi, L., and Sardella, A., 1973, *Geologia della zona compresa
930 fra Bisaccia (Av): Memorie della Societa Geologica Italiana*, v. 12, p. 279-315.
- 931 Ciarapica, G., and Passeri, L., 2002, The palaeogeographic duplicity of the Apennines: *Bollettino della
932 Societa geologica italiana*, v. 121, p. 67-75.
- 933 CIESM, 2008, *The Messinian Salinity Crisis from mega-deposits to microbiology- A consensus report:
934 CIESM workshop Monograph* [F. Briand, Ed.], v. 33, p. 168p.
- 935 Cippitelli, G., 2007, The CROP-04 seismic profile. Interpretation and structural setting of the Agropoli-
936 Barletta Geotraverse: *Bollettino della Societa Geologica Italiana*, v. 7, p. 267-281.

- 937 Chiocchini, U., Madonna, S., Barbieri, M., Si Stefano, A., Le Pera, E., and Potetti, M., 2003, Le unita
938 tardo orogene dell'area tra Benevento ed Avellino (Appennino Campano): In: Studi Geologici
939 Camerti, numero speciale Edimont, Citta di Castello (PG), p. 49-62.
- 940 Chorowicz, J., Cadet, J.-P., and Stephan, J.-F., 1981, Le secteur transversal de Scutari-Pec: apports de
941 l'étude de la fracturation à partir des données landsat: Bulletin de la société géologique de
942 France, v. 18, p. 217-228.
- 943 Clauzon, G., Rubino, J.-L., and Casero, P., 1997, Regional modalities of the Messinian Salinity Crisis in
944 the framework of a two phases model. : R.C.M.N.S. Interim-Colloquium, Catane, p. 44-46.
- 945 Clauzon, G., Suc, J.P., Gautier, F., Berger, A., and Loutre, M.F., 1996, Alternate interpretation of the
946 Messinian salinity crisis: controversy resolved? : *Geology*, v. 24 p. 363-366.
- 947 Clauzon G., Suc J.-P., Do Couto D., Jouannic G., Melinte-Dobrinescu M.C., Jolivet L., Quillévère F.,
948 Lebreton N., Mocochain L., Popescu S.-M., Martinell J., Doménech R., Rubino J.-L., Gumiaux C.,
949 Warny S., Bellas S.M., Gorini C., Bache F., Rabineau M., and Estrada F., 2015. New insights on
950 the Sorbas Basin (SE Spain): The onshore reference of the Messinian Salinity Crisis. *Marine and
951 Petroleum Geology*, 66, 71-100.
- 952 Colalongo, M.L., Cremonini, G., Farabegoli, E., Sartori, R., Tampieri, R., Tomadin, L., 1976. Palaeoen-
953 vironmental study of the "Colombacci" Formation in Romagna (Italy): the Cella section. *Mem-
954 orie della Società Geologica Italiana* 16, 197-216.
- 955 Corrado, S., Aldega, L., Di Leo, P., Giampaolo, C., Invernizzi, C., Mazzoli, S., and Zattin, M., 2005,
956 Thermal maturity of the axial zone of the southern Apennines fold-and-thrust belt (Italy) from
957 multiple organic and inorganic indicators: *Terra Nova*, v. 17, p. 56-65.
- 958 Corradini, D., and Biffi, U., 1988, Dinocyst study at the Messinian-Pliocene boundary in the Cava Ser-
959 redi section, Tuscany, Italy: *Bulletin des Centres de Recherches Exploration-Production Elf-
960 Aquitaine*, v. 12, p. 221-236.
- 961 Cosentino, D., Buchwaldt, R., Sampalmieri, G., Ladanza, A., Cipollari, P., Schildgen, T.F., Hinnov,
962 L.A., Ramezani J., and Bowering, S.A., 2013, Refining the Mediterranean "Messinian gap" with
963 high-precision U-Pb zircon geochronology, central and northern Italy: *Geology*, v. 41, p. 323-
964 326.
- 965 Corselli, C., and Grecchi, G., 1984. The passage from hypersaline to hyposaline conditions in the Medi-
966 terranean Messinian: discussion of the possible mechanisms triggering the "Lago Mare" facies.
967 *Pale´obiologie continentale* 14 (2), 225-239.
- 968 De Alteriis, G., 1995, Different foreland basins in Italy: examples from the central and southern Adriat-
969 ic Sea: *Tectonophysics*, v. 252, p. 349-373.
- 970 DeCelles, P., and Cavazza, W., 1995, Upper Messinian fan conglomerates in eastern Calabria (southern
971 Italy): response to microplate migration and Mediterranean sea-level changes: *Geology*, v.23,
972 p.775-778.
- 973 Dellong, D., Klingelhoefer, F., Kopp, H., Graindorge, D., Margheriti, L., Moretti, M., Murphy, S., and
974 Gutcher, M.-A., 2018, Crustal structure of the Ionian basin and eastern Sicily margin: Results
975 from a wide-angle seismic survey: *Journal of Geophysical Research: Solid Earth*, v. 123.
- 976 Del Olmo, W.M., 2011, The Messinian in the Gulf of Valencia and Alboran Sea (Spain): paleogeogra-
977 phy and paleoceanography implications: *Revista de la Sociedad Geológica de España*, v. 24, p. 1-
978 22.
- 979 Del Olmo, M.W., and Comas, M., 2008, Arquitectura sísmica, olistostromas y fallas extensionales en el
980 norte de la cuenca oeste del mar de Alborán. : *Revista de la Sociedad Geológica de España*, v.
981 21, p. 151-167.
- 982 Dercourt, J., and Fleury, J.J., 1972, The Canadian Cordillera, the Hellenides, and the Sea-floor
983 Spreading theory: *Canadian Journal of Earth Sciences*, v. 9, p. 709-743.
- 984 Di Nocera, S., Matano, F., Pescatore, T., Pinto, F., Quarantiello, R., Senatore, M.R., and Torre, M.,
985 2006, Schema geologico del transetto Monti Picentini orientali-Monti della Daunia meridionali:
986 unita stratigrafiche ed evoluzione tettonica del settore esterno dell' Appennino meridionale: *Bol-
987 letino della Società Geologica Italiana*, v. 125, p. 39-58.

- 988 Do Couto, D., Gorini, C., Jolivet, L., Lebret, N., Augier, R., Gumiaux, C., d'Acremont, E., Ammar, A.,
989 Jabour, H., and Auxietre, J.-L., 2016, Tectonic and stratigraphic evolution of the Western Al-
990 boran Sea Basin in the last 25Myrs: Tectonophysics, v. 677-678, p. 280-311.
- 991 Do Couto D., Popescu S.-M., Suc J.-P., Melinte-Dobrinescu M.C., Barhoun N., Gorini C., Jolivet L.,
992 Poort J., Jouannic G., and Auxietre J.-L., 2014. Lago Mare and the Messinian Salinity Crisis: Ev-
993 idences from the Alboran Sea (S. Spain). *Marine and Petroleum Geology*, 52, 57-76.
- 994 El Euch-El Kundi, N., Ferry, S., Suc, J.-P., Clauzon, G., Melinte-Dobrinescu, M.C., Gorini, C., Safra, A.,
995 Zargouni, F., 2009, Messinian deposits and erosion in northern Tunisia: inferences on Strait of
996 Sicily during the Messinian Salinity Crisis: *Terra Nova*, v. 21, p. 41-48.
- 997 Elter, P., Giglia, G., Tongiorgi, M., and Trevisan, L., 1975, Tensional and compressional areas in the
998 recent (Tortonian to Present) evolution of the Northern Apennines: *Bollettino di Geofisica Te-
999 orica ed Applicata*, v. 17, p. 3-18.
- 1000 Esu, D., 2007, Latest Messinian "Lago-Mare" Lymnocardiinae from Italy: Close relations with the Pon-
1001 tian fauna from the Dacic Basin: *geobios*, v. 40, p. 291-302.
- 1002 Esu, D., Taviani, M., 1989. Oligohaline mollusc fauna of the Colombacci Formation (upper Messinian)
1003 from an exceptional fossil vertebrate site in the Romagna Apennines: Monticino Quarry
1004 (Brisighella, N Italy). *Bollettino della Societa` Paleontologica Italiana* 28, 265-270.
- 1005 Fantoni, R., and Franciosi, R., 2008, 8 geological sections crossing Po Plain and Adriatic foreland: Ri-
1006 assunti dell'84°. Congresso Nazionale Sassari 15-17 settembre 2008. *Rend online Societa Geo-
1007 logica Italia*, v. 3, p. 367-368.
- 1008 Fantoni, R., and Franciosi, R., 2010, Tectono-sedimentary setting of the Po Plain and Adriatic foreland:
1009 *Rend. Fis. Acc. Lincei*, p. 197-209.
- 1010 Faranda, C., Gliozzi, E., Ligios, S., 2007. Late Miocene brackish Loxoconchidae (Crustacea, Ostracoda)
1011 from Italy. *Geobios* 40, 303-324.
- 1012 Fauquette, S., Bernet, M., Suc, J.-P., Grosjean, A.-S., Guillot, S., van der Beek, P., Jourdan, S., Popescu,
1013 S.-M., Jimenez-Moreno, G., Bertini, A., Pittet, B., Tricart, P., Dumont, T., Schwartz, S., Zheng,
1014 Z., Roche, E., Pavia, G., Gardien, V., 2015a. Quantifying the Eocene to Pleistocene topographic
1015 evolution of the southwestern Alps, France and Italy. *Earth and Planetary Science Letters* 412,
1016 220-234.
- 1017 Fauquette, S., Bertini, A., Manzi, V., Roveri, M., Argnani, A., Menichetti, E., 2015b. Reconstruction of
1018 the Northern and Central Apennines (Italy) palaeoaltitudes during the late Neogene from pol-
1019 len data. *Review of Palaeobotany and Palynology* 218, 117-126.
- 1020 Festa, V., Teofilo, G., Tropeano, M., Sabato, L., and Spalluto, L., 2013, New insights on diapirism in
1021 the Adriatic Sea: the Tremiti salt structure (Apulia offshore, southeastern Italy): *Terra Nova*, v.
1022 0, p. 1-10.
- 1023 Fidalgo-González, L., 2001, La cinématique de l'Atlantique Nord: la question de la déformation intra-
1024 plaque: Thèse de doctorat de l'Université de Bretagne Occidentale, Brest.
- 1025 Finetti, I.R., 1982, Structure, stratigraphy and evolution of central Mediterranean: *Bollettino Di Geofisi-
1026 ca Teorica Ed Applicata*, v. 24, p. 247-312.
- 1027 Flecker, R., Krijgsman, W., Capella, W., de Castro Martins, C., Dmitriev, E., Mayser, J.-P., Marzocchu,
1028 A., Modestu, S., Ochoa, D., Simon, D., Tulbure, M., van der Berg, B., van der Schreef, M., de
1029 Lange, G., Ellam, R., Govers, R., Gutjah, M., Hilgen, F., Kouwenhoven, T.J., Lofi, J., Meijer, P.,
1030 Sierro, F.J., Bachiri, N., Barhoun, N., Alami, A.C., Chacon, B., Flores, J.A., Gregory, J., How-
1031 ard, J., Lunt, D., Ochoa, M., Pancost, R., Vincent, S., and Yousfi, M.Z., 2015, Evolution of the
1032 Late Miocene Mediterranean-Atlantic gateways and their impact on regional and global envi-
1033 ronmental change: *Earth-Science Reviews*, v. 150, p. 365-392.
- 1034 Fontes, J.-C., Filly, A., Gaudant, J., 1987. Conditions de dépôt du Messinien évaporitique des environs
1035 d'Alba (Piémont) : arguments paléontologiques et isotopiques. *Bollettino della Societa` Paleon-
1036 tologica Italiana* 26, 199-210.
- 1037 Frasheri, A., Bushati, S., and Bare, V., 2009, Geophysical outlook on structure of the Albanids: *Journal
1038 of the Balkan Geophysical Society*, v. 12, p. 9-30.

- 1039 Frasher, A., Nishani, P., and Bushati, S., 1996, Relationship between tectonic zones of the Albanids,
1040 based on results of geophysical studies: Peri Tethys Memoir 2: Structure and Prospects of Alpine
1041 Basins and Forelands.: *Hist. Nat.*, v. 170, p. 485-511.
- 1042 Funicello, R., Montone, P., Parotto, M., Salvini, F., and Tozzi, M., 1991, Geodynamical evolution of an
1043 intra-orogenic foreland: The Apulia case history (Italy). *Bolletino della Società Geologica Ital-*
1044 *iana*, v. 110, p. 419-425.
- 1045 Garcia, M., Maillard, A., Aslanian, D., Rabineau, M., Alonso, B., Gorini, C., and Estrada, F., 2011, The
1046 Catalan margin during the Messinian Salinity Crisis: Physiography, morphology and sedimentary
1047 record: *Marine Geology*, v. 284, p. 158-174.
- 1048 Garcia-Castellanos, D., Estrada, F., Jiménez-Munt, L., Gorini, C., Fernandez, M., Vergès, J., and De
1049 Vicente, R., 2009, Catastrophic flood of the Mediterranean after the Messinian salinity crisis:
1050 *Nature*, v. 462, p. 778-781.
- 1051 Garcia-Castellanos, D., Micallef, A., Estrada, F., Camerlenghi, A., Ercilla, G., Periañez, R., and Abril,
1052 J.M., 2020, The Zanclean megaflood of the Mediterranean—Searching for independent evidence:
1053 *Earth Science Reviews*, v. 201.
- 1054 Gargani, J., Rigollet, C., and Scarselli, S., 2010, Isostatic response and geomorphological evolution of
1055 the Nile valley during the Messinian salinity crisis: *Bull Soc. Géol. France*, v. 181, p. 19-26.
- 1056 Gattacceca, J., and Speranza, F., 2002, Paleomagnetism of Jurassic to Miocene sediments from the Ap-
1057 peninic carbonate platform (southern Apennines, Italy) : evidence for a 60° counterclockwise
1058 Miocene rotation: *Earth and planet. Sci. Lett.*, v. 201, p. 19-34.
- 1059 Giaconia, F., Booth-Rea, G., Ranero, C.R., Gracia, E., Bartolome, R., Calahorrano, A., Lo Iacono, C.,
1060 Vendrell, M.G., Cameselle, A.L., Coasta, S., Gomez de la Peña, L., Martinez-Loriente, S., Perea,
1061 H., and Viñas, M., 2015, Compressional tectonic inversion of the Algero-Balearic basin: Late-
1062 most Miocene to present oblique convergence at the Palomares margin (Western Mediterranean):
1063 *Tectonics*, v. 34.
- 1064 Gillet, S., 1968. La faune messinienne des environs d'Ancona avec une notice géologique par E. Ce-
1065 retti. *Giornale di Geologia* 36 (1-4), 69-100.
- 1066 Ghielmi, M., Minervini, M., Nini, C., Rogledi, S., Rossi, M., and Vignolo, A., 2010, Sedimentary and
1067 tectonic evolution in the eastern Po-Plain and northern Adriatic Sea area from Messinian to
1068 Middle Pleistocene (Italy): *Rend. Fis. Acc. Lincei*, v. 21, p. 131-166.
- 1069 Ghielmi, M., Minervini, M., Nini, C., Rogledi, S., and Rossi, M., 2013, Late Miocene - Middle Pleisto-
1070 cene Sequences In The Po-Plain - Northern Adriatic Sea (Italy): The Stratigraphic Record Of
1071 Modification Phases Affecting A Complex Foreland Basin: *Marine and Petroleum Geology*, v.
1072 42, p. 50-51.
- 1073 Gliozzi, E., Ceci, M.E., Grossi, F., and Ligios, S., 2007, Paratethyan Ostracod immigrants in Italy during
1074 the Late Miocene: *geobios*, v. 40, p. 325-337.
- 1075 Gorini, C., Montadert, L., and Rabineau, M., 2015, New imaging of the salinity crisis: Dual Messinian
1076 lowstand megasequences recorded in the deep basin of both the eastern and western Mediterra-
1077 nean: *Marine and Petroleum Geology*, p. 1-17.
- 1078 Govers, R., Meijer, P., and Krijgsman, W., 2009, Regional isostatic response to Messinian Salinity Crisis
1079 events: *Tectonophysics*, v. 463, p. 109-129.
- 1080 Grubic, A., and Marovic, M., 1991, Tectonic features and genesis of the Scutari-Pec transverse in the
1081 Morka Gora area, Yugoslavia: *Géologie Méditerranéenne*, v. 18, p. 163-170.
- 1082 Gutcher, M.A., Kopp, H., Krastel, S., Bohrmann, G., Garlan, T., Zaragosi, S., Klaucke, I., Wintersteller,
1083 P., Loubrieu, B., Le Faou, Y., San Pedro, L., Dominguez, S., Rovere, M., Mercier De Lepinay,
1084 B., Ranero, C., and Sallares, V., 2017, Active tectonics of the Calabrian subduction revealed by
1085 new multi-beam bathymetric data and high-resolution seismic profiles in the Ionian Sea (Central
1086 Mediterranean): *Earth and Planetary Science Letters*, v. 461, p. 61-72.
- 1087 Hairabian, A., Borgomano, J., Masse, J.-P., and Nardon, S., 2015, 3-D stratigraphic architecture, sedi-
1088 mentary processes and controlling factors of Cretaceous deep-water resedimented carbonates
1089 (Gargano Peninsula, SE Italy): *Sedimentary Geology*, v. 317, p. 116-136.

- 1090 Handy, M.R., M. Schmid, S., Bousquet, R., Kissling, E., and Bernoulli, D., 2010. Reconciling plate-
1091 tectonic reconstructions of Alpine Tethys with the geological-geophysical record of spreading
1092 and subduction in the Alps: *Earth-Science Reviews*, v. 102, p. 121-158.
- 1093 Henriquet, M., Dominguez, S., Barreca, G., Malavieille, J., and Monaco, C., 2020, Structural and tec-
1094 tono-stratigraphic review of the Sicilian orogen and new insights from analogue modeling:
1095 *Earth-Science Reviews*, v. 208.
- 1096 Hilgen, F., Kuiper, K., Krijgsman, W., Snel, E., and Laan, E.V.D., 2007, Astronomical tuning as the
1097 basis for high resolution chronostratigraphy : the intricate history of the messinian salinity crisis:
1098 *Stratigraphy*, v. 4, p. 231-238.
- 1099 Hsü, K., Montadert, L., Bernouilli, D., Bizon, G., Cita, M., Erickson, A., Fabricius, F., Garrison, R.E.,
1100 Kidd, R.B., Mélières, F., Müller, C., and Wright, R.C., 1978, Initial Reports of the Deep Sea
1101 Drilling Project, DSDP Volume XLII.
- 1102 Iaccarino, S.M., Bertini, A., Di Stefano, A., Ferraro, L., Gennari, R., Grossi, F., Lirer, F., Manzi, V.,
1103 Menichetti, E., Ricci Lucchi, F., Taviani, M., sturiale, G., and Angeletti, L., 2008, The Trave
1104 section (Monte dei Corvi, Ancona, Central Italy): an integrated paleontological study of the
1105 Messinian deposits: *Stratigraphy*, v. 5, p. 281-306.
- 1106 Kiliyas, A., Tranos, M., Mountrakis, D., Shallo, M., Marto, A., and Turku, I., 2001, Geometry and kin-
1107 ematics of deformation in the Albanian orogenic belt during the Tertiary.: *Journal of Ge-*
1108 *odynamics*, v. 31, p. 169-187.
- 1109 Korbar, T., 2009, Orogenic evolution of the External Dinarides in the NE Adriatic region: a model
1110 constrained by tectonostratigraphy of Upper Cretaceous to Paleogene carbonates: *Earth Science*
1111 *Reviews*, v. 96, p. 296-312.
- 1112 Krijgsman, W., Garcès, M., Langereis, C.G., Daams, R., van Dam, J., van der Meulen, A.J., Agusti, J.,
1113 and CABrera, L., 1996, A new chronology for the middle to late Miocene continental record in
1114 Spain: *Earth and planet. Sci. Lett.*, v. 142, p. 367-380.
- 1115 Krijgsman, W., Leewis, M.E., Garcès, M., Kouwenhoven, T.J., Kuiper, K.F., and Sierro, F.J., 2006, Tec-
1116 tonic control for evaporite formation in the Eastern Betics (Tortonian; Spain): *Sedimentary ge-*
1117 *ology*, v. 188-189, p. 155-170.
- 1118 Leeever, K.A., Matenco, L., Garcia-Castellanos, D., and Cloetingh, S., 2010, The evolution of the Dan-
1119 ube gateway between Central and Eastern Paratethys (SE Europe): Insight from numerical mod-
1120 elling of the causes and effects of connectivity between basins and its expression in the sedimen-
1121 tary record: *Tectonophysics*, v. 502, p. 175-195.
- 1122 Leroux, E., Aslanian, D., Rabineau, M., Moulin, M., Granjeon, D., Gorini, C., and Droz, L., 2015a,
1123 Sedimentary markers in the Provençal Basin (western Mediterranean): a window into deep geo-
1124 dynamic processes: *Terra Nova*, v. 27, p. 122-129.
- 1125 Leroux, E., Rabineau, M., Aslanian, D., Gorini, C., Bache, F., Moulin, M., Pellen, R., Granjeon, D.,
1126 and Rubino, J.-L., 2015b, Post-rift evolution of the Gulf of Lion margin tested by stratigraphic
1127 modelling: *Bulletin de la société géologique de france*, v. 186, p. 291-308.
- 1128 Leroux, E., Rabineau M., Aslanian D., Gorini C., Molliex S., Bache F., Robin C., Droz L., Moulin M.,
1129 Poort J., Rubino J.-L., Suc J.-P., 2017. High resolution evolution of terrigenous sediment yields
1130 in the Provence Basin during the last 6 Ma: relation with climate and tectonics: *Basin Research*,
1131 v. 29 (3), p.305-339
- 1132 Leroux, E., Aslanian, D., Rabineau, M., Pellen, R., and Moulin, M., 2018, The late Messinian event: a
1133 worldwide tectonic upheaval: *Terra Nova*, v. 30, p. 207-214.
- 1134 Lofi, J., 2018, Seismic Atlas of the Messinian Salinity Crisis markers in the Mediterranean Sea - Volume
1135 2: Commission for the Geological Map of the World. Société Géologique de France, v. 2, p. 1-
1136 72.
- 1137 Lofi, J., Sage, F., Deverchère, J., Loncke, L., Maillard, A., Gaullier, V., Thinon, I., Gillet, H., Guennoc,
1138 P., and Gorini, C., 2011, Refining our knowledge of the Messinian Salinity crisis records in the
1139 offshore domaine through multi-site seismic analysis: *Bulletin de la société géologique de france*,
1140 v. 182, p. 163-180.

- 1141 Lugli, S., Manzi, V., Roveri, M., and Schreiber, B.C., 2010, The Primary Lower Gypsum in the Mediter-
1142 ranean: a new facies interpretation for the first stage of the Messinian salinity crisis.: *Palaeogeog-*
1143 *raphy, Palaeoclimatology, Palaeoecology*, v. 297, p. 83-99.
- 1144 Lymer, G., Lofi, J., Gaullier, V., Maillard, A., Thinon, I., Sage, F., Chanier, F., and Vendeville, B.C.,
1145 2018, The Western Tyrrhenian Sea revisited: New evidence for a rifted basin during the Mes-
1146 sinian Salinity Crisis: *Marine Geology*, v. 398, p. 1-21.
- 1147 Madof, A.S., Bertoni, C., and Lofi, J., 2019, Discovery of vast fluvial deposits provides evidence for
1148 drawdown during the late Miocene Messinian salinity crisis: *Geology*, v. 47, p. 171-174.
- 1149 Maillard, A., Gorini, C., Mauffret, A., Sage, F., Lofi, J., and Gaullier, V., 2006, Offshore evidence of
1150 polyphase erosion in the Valencia Basin (Northwestern Mediterranean): Scenario for the Mes-
1151 sinian Salinity Crisis.: *Sedimentary Geology*, v. 188-189, p. 69-91.
- 1152 Manzi, V., Argnani, A., Corcagnani, A., Lugli, S., and Roveri, M., 2020, The Messinian salinity crisis in
1153 the Adriatic foredeep: Evolution of the largest evaporitic marginal basin of the Mediterranean:
1154 *Marine and Petroleum Geology*, v. 115.
- 1155 Manzi, V., Gennari, R., Hilgen, F., Krijgsman, W., Lugli, S., Roveri, M., and Sierro, F.J., 2013, Age re-
1156 finement of the Messinian salinity crisis onset in the Mediterranean: *Terra Nova*, v. 25, p. 315-
1157 322.
- 1158 Manzi, V., Gennari, R., Lugli, S., Persico, D., Regheizzi, M., Roveri, M., Schreiber, B.C., Calvo, R.,
1159 Gavrieli, I., and Gvirtzman, Z., 2018, The onset of the Messinian salinity crisis in the deep East-
1160 ern Mediterranean basin: *Terra Nova*, v. 38, p. 42-49.
- 1161 Manzi, V., Roveri, M., Gennari, R., Bertini, A., Biffi, U., Giunta, S., Iaccarino, S.M., Lanci, L., Lugli, S.,
1162 Negri, A., Riva, A., Rossi, M.E., and Taviani, M., 2007, The deep-water counterpart of the Mes-
1163 sinian Lower Evaporites in the Apennine foredeep: The Fananello section (Northern Apen-
1164 nines, Italy): *Palaeogeography, Palaeoclimatology, Palaeoecology*.
- 1165 Masters, J.C., Génin, F., Zhang, Y., Pellen, R., HUck, T., Mazza, P.P.A., Rabineau, M., Doucouré, M.,
1166 and Aslanian, D., 2020, Biogeographic mechanisms involved in the colonization of Madagascar
1167 by African vertebrates: Rifting, rafting and runways: *Journal of Biogeography*, p. 1-19.
- 1168 Matano, F., 2007, The 'Evaporiti di Monte Castello' deposits of the Messinian Southern Apennines
1169 foreland basin (Irpinia-Daunia Mountains, Southern Italy): stratigraphic evolution and geologi-
1170 cal context: Schreiber, B. C., Lugli, S. & Babel, M. (eds) *Evaporites Through Space and Time*.
1171 Geological Society, London, Special Publications, v. 285, p. 191-218.
- 1172 Matano, F., Barbieri, M., Di Nocera, S., and Torre, M., 2005, Stratigraphy and strontium geochemistry
1173 of Messinian evaporite-bearing successions of the southern Apennines foredeep, Italy: implica-
1174 tions for the Mediterranean "salinity crisis" and regional palaeogeography: *Palaeogeography, Pal-*
1175 *aeoclimatology, Palaeoecology*, v. 217, p. 87-114.
- 1176 Matano, F., Critelli, S., Barone, M., Muto, F., and Di Nocera, S., 2014, Stratigraphic and provenance
1177 evolution of the Southern Apennines foreland basin system during the Middle Miocene to Plio-
1178 cene (Irpinia-Sannio successions, Italy): *Marine and Petroleum Geology*, v. 57, p. 652-670.
- 1179 Matias, L., Olivet, J.-L., Aslanian, D., and Fidalgo, L., 2005, PLACA: a white box for plate reconstruc-
1180 tion and best-fit pole determination: *Computer & Geosciences*, v. 31, p. 437-452.
- 1181 Mazzoli, S., D'Errico, M., Aldega, L., Corrado, S., Invernizzi, C., Shiner, P., and Zattin, M., 2008, Tec-
1182 tonic burial and "young" (<10 Ma) exhumation in the southern Apennines fold-and-thrust belt
1183 (Italy): *Geological Society of America*, v. 36, p. 243-246.
- 1184 Mele, G., 2001, The Adriatic lithosphere is a promontory of the African plate: Evidence of a continuous
1185 mantle lid in the Ionian Sea from efficient Sn propagation: *Geophysical Research Letters*, v. 28,
1186 p. 431-434.
- 1187 Micallef, A., Camerlenghi, A., Garcia-Castellanos, D., Otero, D.C., Gutscher, M.-A., Barreca, G., Spa-
1188 tola, D., Facchin, L., Geletti, R., Krastel, S., Gross, F., and Urlaub, M., 2018, Evidence of the
1189 Zanclean megaflood in the eastern Mediterranean basin: *Nature Scientific Reports*, v. 8.
- 1190 Milli, S., Moscatelli, M., Stanzione, O., Falcini, F., and Bigi, S., 2006, The Messinian Laga Formation,
1191 facies, geometries, stratigraphic architecture and structural style of a confined turbidite basin
1192 (Central Apennines, Italy). *Excursion Guidebook, Field Trip 17-21 Settembre 2006*.

- 1193 Milli, S., Moscatelli, M., Stanzione, O., and Falcini, F., 2007, Sedimentology and physical stratigraphy of
1194 the Messinian turbidite deposits of the Laga Basin (central Apennines, Italy): *Bolletino della So-*
1195 *cietà Paleontologica Italiana*, v. 126, p. 255-281.
- 1196 Morelli, D., 2002, Evoluzione tettonico-stratigrafica del Margine Adriatico compreso tra il Promontorio
1197 garganico e Brindisi: *Memoria di Società Geologica Italia*, v. 57, p. 343-353.
- 1198 Moscardelli, L., and Wood, L., 2007, New classification system for mass transport complexes in offshore
1199 Trinidad: *Basin Research*, v. 20, p. 73-98.
- 1200 Moulin, M., Klingelhoefer, F., Afilhado, A., Aslanian, D., Schnurle, P., Nouzé, H., Rabineau, M.,
1201 Beslier, M.-O., and Feld, A., 2015, Deep crustal structure across a young passive margin from
1202 wide-angle and reflection seismic data (The SARDINIA Experiment) - I. Gulf of Lion's margin:
1203 *Bulletin de la société géologique de France*, v. 186, p. 309-330.
- 1204 Ori, G.G., Serafini, G., Visentin, C., Ricci Lucchi, F., Casnedi, R., Colalongo, M.L., and Mosna, S.,
1205 1991, The Pliocene-Pleistocene Adriatic Foredeep (Marche and Abruzzo, Italy): an integrated
1206 approach to surface and subsurface geology.: In: *Agip-EAPG (Ed.), 3rd EAPG Conference.*
1207 *Adriatic Foredeep Field Trip, Florence May 26-30*, p. 85.
- 1208 Palcu, D.V., Golovina, L.A., Vernyhorova, Y.V., Popov, S.V., and Krijgsman, W., 2017, Middle Mio-
1209 cene paleoenvironmental crises in Central Eurasia caused by changes in marine gateway config-
1210 uration: *Global and Planetary Change*, v. 158, p. 57-71.
- 1211 Panza, G.F., Pontevivo, A., Chimera, G., Raykova, R., and Aoudia, A., 2003, The lithosphere-
1212 asthenosphere: Italy and surroundings: *Episodes*, v. 26, p. 168-173.
- 1213 Pashko, P., and Aliaj, S., 2020, Stratigraphy and tectonic evolution of late Miocene-Quaternary basins in
1214 Eastern Albania: a review: *Bulletin Geological Society of Greece*, v. 56, p. 317-351.
- 1215 Patacca, E., Scandone, P., and Mazza, P., 2008, Oligocene migration path for Apulia macromammals:
1216 the Central-Adriatic bridge: *Bollettino della Società Geologica Italiana*, v. 127, p. 337-355.
- 1217 Pedley, M., Grasso, M., Maniscalco, R., and Esu, D., 2007, The Monte Carrubba Formation (Messinian,
1218 Sicily) and its correlatives: New light on basin-wide processes controlling sediment and biota dis-
1219 tributions during the Palaeomediterranean - Mediterranean transition: *Palaeogeography Palaeo-*
1220 *climatology Palaeoecology*, v. 253, p. 363-384.
- 1221 Pelleau, P., Aslanian, D., Matias, L., Moulin, M., Augustin, J.-M., Quemener G. & Poncelet C., 2015.
1222 Placa4D freeware: a new interactive tool for palinspastic reconstruction in 3D, *AAPG congres*,
1223 *Lisbonne*.
- 1224 Pellen, R., 2016, Géodynamique et impact de la crise d'érosion et de salinité Messinienne sur les trans-
1225 ferts sédimentaires (bassin de Valence, bassin Adriatique): Thèse de doctorat - Sciences de la
1226 Terre. Université Bretagne Occidentale, p. 550 p.
- 1227 Pellen, R., Aslanian, D., Rabineau, M., Suc, J.P., Gorini, C., Leroux, E., Blanpied, C., Silenziario, C.,
1228 Popescu, S.-M., and Rubino, J.L., 2019, The Messinian Ebro River incision: *Global and Pla-*
1229 *netary Change*, v. 181.
- 1230 Pellen, R., Aslanian, D., Rabineau, M., 2021. A comprehensive compilation of the seismic stratigraphy
1231 markers along the Adriatic Sea. *SEANOE*. <https://doi.org/10.17882/84576>
- 1232 Pellen, R., Popescu, S.-M., Suc, J.P., Melinte-Dobrinescu, M.C., Rubino, J.-L., Rabineau, M., Marabini,
1233 S., Loget, N., Casero, P., Cavazza, W., Head, M.J., and Aslanian, D., 2017, The Apennine fore-
1234 deep (Italy) during the latest Messinian: Lago Mare reflects competing brackish and marine
1235 conditions based on calcareous nannofossils and dinoflagellate cysts: *Geobios*, v. 50, p. 237-
1236 257.
- 1237 Pescatore, T.S., Di Nocera, S., Matano, F., Pinto, F., Boiano, U., Civile, D., Martino, C., and Quarantiello,
1238 R., 2008, Prime considerazioni sulla geologia del settore centrale dei monti del Sannio:
1239 *Memorie Descr. Carta Geol. It.*, v. 77, p. 77-94.
- 1240 Petruccio, A.V., Agosta, F., Prosser, G., and Rizzo, E., 2017, Cenozoic tectonic evolution of the northern
1241 Apulian carbonate Platform (southern Italy): *Italian Journal of Geosciences*, v. 136, p. 1-16.
- 1242 Popescu S.-M., Dalibard M., Suc J.-P., Barhoun N., Melinte-Dobrinescu M.C., Bassetti M.A., Deaconu
1243 F., Head M.J., Gorini C., Do Couto D., Rubino J.-L., Auxietre J.-L., Floodpage J., 2015. Lago
1244 Mare episodes around the Messinian-Zanclean boundary in the deep southwestern Mediterra-
1245 nean. *Marine and Petroleum Geology*, 66, 1, 55-70.

- 1246 Popescu, S.M., Melinte, M.-C., Suc, J.-P., Clauzon, G., Quillévéré, F., and Sütö-Szentai, M., 2007, Earliest
1247 Zanclean age for the Colombacci and uppermost Di Tetto formations of the “latest Messinian”
1248 northern Apennines: New palaeoenvironmental data from the Maccarone section (Marche
1249 Province, Italy): *Geobios*, v. 40, p. 359-373.
- 1250 Popescu, S.M., Melinte, M.-C., Suc, J.-P., Clauzon, G., Quillévéré, F., Sütö-Szentai, M., 2008, Comment
1251 on Marine reflooding of the Mediterranean after the Messinian Salinity Crisis predates the Zanclean
1252 GSSP. Reply to the “Comment on ‘Earliest Zanclean age for the Colombacci and uppermost
1253 Di Tetto formations of the “latest Messinian” northern Apennines: New palaeoenvironmental
1254 data from the Maccarone section (Marche Province, Italy)’ by Popescu *et al.* (2007) *Geobios*
1255 40 (359–373)” authored by Roveri *et al.*: *Geobios*, v. 41, p. 657-660.
- 1256 Popescu, S.-M., Cavazza, W., Suc, J.-P., Melinte-Dobrinescu, M.C., Barhoun, N., and Gorini, C., 2021,
1257 Pre-Zanclean end of the Messinian Salinity Crisis: new evidence from central Mediterranean
1258 reference sections: *Journal of the Geological Society*, v. 178, p. 1-16.
- 1259 Rabineau, M., Leroux, E., Bache, F., Aslanian, D., Gorini, C., Moulin, M., Molliex, S., Droz, L., Reis,
1260 T.D., Rubino, J.-L., and Olivet, J.-L., 2014, Quantifying subsidence and isostatic readjustment
1261 using sedimentary paleomarkers, example from the Gulf of Lion: *Earth and Planetary Science
1262 Letters*, v. 388, p. 1-14.
- 1263 Ricci Lucchi, F., 1986, The Oligocene to Recent foreland basins of the northern Apennines: *Spec.
1264 Publ. int. Ass. Sediment*, v. 8, p. 105-139.
- 1265 Riguzzi, F., and Doglioni, C., 2020, Gravity and crustal dynamics in Italy: *Rendiconti Lincei. Scienze
1266 Fisiche e Naturali* volume, v. 31, p. 49-58.
- 1267 Ritzwoller, M.H., Yang, Y., Richmond, R.M., Pasyanos, M.E., Villasenor, A., Levin, V., Hofstetter, R.,
1268 Pinsky, V.I., Kraeva, N.V., and Lerner-Lam, A., 2007, Short Period Surface Wave Dispersion
1269 Across the Mediterranean Region: Improvements Using Regional Seismic Networks: 29th Monitoring
1270 Research Review: Ground-Based Nuclear Explosion Monitoring Technologies. Conference
1271 paper.
- 1272 Rossi, M., Minervini, M., Ghielmi, M., and Rogledi, S., 2015, Messinian and Pliocene erosional surfaces
1273 in the Po Plain-Adriatic Basin: Insights from allostratigraphy and sequence stratigraphy in assessing
1274 play concepts related to accommodation and gateway turnarounds in tectonically active
1275 margins: *Marine and Petroleum Geology*, v. 66, p. 192-216.
- 1276 Roure, F., Casero, P., and Addoum, B., 2012, Alpine inversion of the North African margin and
1277 delamination of its continental lithosphere: *Tectonics*, v. 31, p. TC3006.
- 1278 Roveri, M., Bassetti, M.A., and Ricci Lucchi, F., 2001, The Mediterranean Messinian Salinity Crisis: an
1279 Apennine foredeep perspective. : *Sedimentary Geology*, v. 140.
- 1280 Roveri, M., Boscolo Gallo, A., Rossi, M., Gennari, R., Iaccarino, S.M., Lugli, S., Manzi, V., Negri, A.,
1281 Rizzini, F., and Taviani, M., 2005, The Adriatic foreland record of Messinian events (Central
1282 Adriatic Sea, Italy): *GeoActa*, v. 4.
- 1283 Roveri, M., Flecker, R., Krijgsman, W., Lofi, J., Lugli, S., Manzi, V., Sierro, F.J., bertini, A., Camerlenghi,
1284 A., De Lange, G., Govers, R., Hilgen, F.J., Hübscher, C., Meijer, P.T., and Stoica, M., 2014,
1285 The Messinian Salinity Crisis: Past and future of a great challenge for marine sciences: *Marine
1286 Geology*, v. 352, p. 25-58.
- 1287 Roveri, M., Gennari, R., Lugli, S., Manzi, V., Minelli, N., Reghezzi, M., Riva, A., Rossi, M.E., and
1288 Schreiber, B.C., 2016, The Messinian salinity crisis: open problems and possible implications
1289 for Mediterranean petroleum systems: *Petroleum Geoscience*.
- 1290 Roveri, M., Landuzzi, A., Bassetti, M.A., Lugli, S., Manzi, V., Ricci Lucchi, F., and Vai, G.B., 2004, The
1291 record of Messinian events in the northern Apennines foredeep basins: Pre-congress guide of
1292 the 32nd International Geological congress v. 2.
- 1293 Roveri, M., Lugli, S., Manzi, V., and Schreiber, B.C., 2008a, The Messinian Sicilian stratigraphy revisited:
1294 new insights for the Messinian salinity crisis: *Terra Nova*, v. 20, p. 483-488.
- 1295 Roveri, M., and Manzi, V., 2006, The Messinian salinity crisis: Looking for a new paradigm?: *Palaeogeography,
1296 Palaeoclimatology, Palaeoecology*, v. 238, p. 386-398.

- 1297 Roveri, M., Manzi V., Bassetti M.A., Merini M., and Ricci Lucchi F., 1998, Stratigraphy of the Messini-
1298 an post-evaporitic stage in eastern-Romagna (northern Apennines, Italy): *Giornale di Geologia*,
1299 v. 60, p. 119-142.
- 1300 Roveri, M., Manzi, V., Gennari, R., Iaccarino, S., and Lugli, S., 2008b, Recent advancements in the
1301 Messinian stratigraphy of Italy and their Mediterranean-scale implications. : *Bolletino della So-*
1302 *cietà Paleontologica Italiana*, v. 47, p. 71-85.
- 1303 Sage, F., Von Gronefeld, G., Déverchère, J., Gaullier, V., Maillard, A., and Gorini, C., 2005, Seismic
1304 evidence for Messinian detrital deposits at the western Sardinia margin, northwestern Mediter-
1305 ranean: *Marine and Petroleum Geology*, v. 22, p. 757-773.
- 1306 Schmid, S.M., Bernouilli, D., Fügenschuh, B., Matenco, L., Schefer, S., Schuster, R., Tischler, M., and
1307 Ustaszewski, K., 2008, The Alpine-Carpathian-Dinaridic orogenic system: correlation and
1308 evolution of tectonic units: *Swiss Journal of Geosciences*, v. 101, p. 139-183.
- 1309 Scisciani, C., and Calamita, F., 2009, Active intraplate deformation within Adria: Examples from the
1310 Adriatic region: *Tectonophysics*, v. 476, p. 57-72.
- 1311 Scrocca, D., 2006, Thrust front segmentation induced by differential slab retreat in the Apennines (Ita-
1312 ly): *Terra Nova*, v. 18, p. 154-161.
- 1313 Selli, R., 1960, Il Messiniano Mayer-Eymar 1867. Proposta di un neostatotipo: *Giornale di Geologia*, v.
1314 28, p. 1-33.
- 1315 Selli, R., 1973, Il Mediterraneo nel Miocene superiore: un mare sovrasalato: *Scienze*, v. 56, p. 20-21.
- 1316 Shiner, P., Beccacini, A., and Mazzoli, S., 2004, Thin-skinned versus thick-skinned structural models for
1317 Apulian Carbonate Reservoirs: constraints from the Val D'Agri Fields: *Marine and Petroleum*
1318 *Geology*, v. 21, p. 805-827.
- 1319 Silo, V., Muska, K., and Silo, E., 2013, Hydrocarbon evaluation aspects in Molasse reservoirs, Vlorë-
1320 Elbasan region, Albania: *Italian Journal of Geosciences*.
- 1321 Sioni, S., 1996, Mer Ionienne et Apulie depuis l'ouverture de l'Océan Alpin. Thèse de Doctorat, Uni-
1322 versité de Bretagne Occidentale.
- 1323 Sprovieri, M., Ribera d'Alcalà, M., Manta, D.S., Bellanca, A., Neri, R., Lirer, F., Taberner, C., Pueyo,
1324 J.J., and Sammartino, S., 2008, Ba/Ca evolution in water masses of the Mediterranean late
1325 Neogene. *Paleoceanography* v. 23.
- 1326 Stampfli, G.M., and Hochard, C., 2009, Plate tectonics of the Alpine realm: Geological Society,
1327 London, Special Publication, v. 327, p. 89-111.
- 1328 Sternai, P., Caricchi, L., Garcia-Castellanos, D., Jolivet, L., Sheldrake, T.E., and Castelltort, S., 2017,
1329 Magmatic pulse driven by sea-level changes associated with the Messinian salinity crisis: *Nature*
1330 *Geoscience*, p. 1-5.
- 1331 Straume, E.T., Gaina, C., Medvedev, S., and Nisancioglu, K.H., 2020, Global Cenozoic Paleobathymetry
1332 with a focus on the Northern Hemisphere Oceanic Gateways: *Gondwana Research*, v. 86, p.
1333 126-143.
- 1334 Sturani, C., 1973. A fossil eel (*Anguilla* sp.) from the Messinian of Alba (Tertiary Piedmontese Basin).
1335 Palaeoenvironmental and palaeogeographic implications. In: Drogger, C.W., Broekman, J.A.,
1336 Hageman, J., Hantelman, J.J., Marks, P., Meulenkamp, J.E., Schmidt, R.R. (Eds.), Messinian
1337 events in the Mediterranean. Koninklijke Nederlandse Akademie Van Wetenschappen. North-
1338 Holland Publishing Company, Amsterdam, London, pp. 243-255.
- 1339 Suc, J.-P., Do Couto, D., Melinte-Dobrinescu, M.C., Macalet, R., Quillévéré, F., Clauzon, G., Csato,
1340 I., Rubino, J.-L., and Popescu, S.-M., 2011, The Messinian Salinity Crisis in the Dacic Basin
1341 (SW Romania) and early Zanclean Mediterranean-Paratethys high sea-level connection. : *Palaeo-*
1342 *geography, Palaeoclimatology, Palaeoecology*, v. 310, p. 256-272.
- 1343 Suc, J.-P., Popescu, S.-M., Do Couto, D., Clauzon, G., Rubino, J.-L., Melinte-Dobrinescu, M.C., Quil-
1344 lévéré, F., Brun, J.-P., Dumurdzanov, N., Zagorchev, I., Lesic, V., Tomic, D., Sokoutis, D., Mey-
1345 er, B., Macalet, R., and Rifelj, H., 2015, Marine gateway vs. fluvial stream within the Balkans
1346 from 6 to 5 Ma: *Marine and Petroleum Geology*, v. 66, p. 231-245.
- 1347 Tondi, E., Piccardi, L., Cacon, S., Kontny, B., and Cello, G., 2005, Structural and time constraints for
1348 dextral shear along the seismogenic Mattinata fault (Gargano, southern Italy): *Journal of Geo-*
1349 *dynamics*, v. 40, p. 134-152.

- 1350 van Hinsbergen, D.J.J., Langereis, C.G., and Meulenkaamp, J.E., 2004, Revision of the timing, magni-
1351 tude and distribution of Neogene rotations in the western Aegean region: *Tectonophysics*, v.
1352 396, p. 1-34.
- 1353 van Hinsbergen, D.J.J., and Schmid, S.M., 2012, Map view restoration of Aegean-West Anatolian accre-
1354 tion and extension since the Eocene: *Tectonics*, v. 31.
- 1355 van Hinsbergen, D.J.J., Torsvik, T.H., Schmid, S.M., Matenco, L.C., Maffione, M., Vissers, R.L.M.,
1356 Gürer, D., and Spakman, W., 2020, Orogenic architecture of the Mediterranean region and
1357 kinematic reconstruction of its tectonic evolution since the Triassic: *Gondwana Research*, v. 81,
1358 p. 79-229.
- 1359 van Hinsbergen, D.J.J., and Schmid, S.M., 2012, Map view restoration of Aegean-West Anatolian
1360 accretion and extension since the Eocene: *Tectonics*, v. 31.
- 1361 Vezzani, F., Festa, A., and Ghisetti, F.C., 2010, *Geology and Tectonic Evolution of the Central-*
1362 *Southern Apennines, Italy: The Geological Society of America, Special Paper*, v. 469, p. 58 pp.
- 1363 Violanti, D., Gallo, L.M., and Rizzi, A., 2007, Foraminiferal assemblages of the Bric della Muda lam-
1364 inites (Nizza Monferrato, Piedmont): proxies of cyclic paleoenvironmental changes in the Lower
1365 Messinian of Northwestern Italy.: *Geobios*, v. 40, p. 281-290.
- 1366 Violanti, D., Dela Pierre, F., Trenkwalder, S., Lozar, F., Clari, P., Irace, A., and D'Atri, A., 2011, Bio-
1367 stratigraphic and palaeoenvironmental analyses of the Messinian/Zanclean boundary and Zan-
1368 clean succession in the Moncucco quarry (Piedmont, northwestern Italy): *Bulletin de la Société*
1369 *Géologique de France*, v. 182, p. 149-162.
- 1370 Vitale, S., and Ciarcia, S., 2013, Tectono-stratigraphic and kinematic evolution of the southern Apen-
1371 nines/Calabria-Peloritani Terrane system (Italy): *Tectonophysics*, v. 583, p. 164-182.
- 1372 Wrigley, R., Hodgson, N. and Esestine, P. 2015, Petroleum geology and hydrocarbon potential of the
1373 Adriatic Basin, offshore Croatia: *Journal of Petroleum Geology*, Vo. 38 (3), pp. 301-316.
- 1374 Zappaterra, E., 1994, Source-Rock distribution model of the Periadriatic region *The American Associa-*
1375 *tion of Petroleum Geologists Bulletin*, v. 78, p. 333-354.
- 1376 Zarccone, G., Petti, F.M., Cillari, A., Di Stefano, P., Guzetta, D., and Nicosia, U., 2010, A possible bridge
1377 between Adria and Africa: New palaeobiogeographic and stratigraphic constraints on the Meso-
1378 zoic palaeogeography of the Central Mediterranean area: *Earth-Science Reviews*, v. 103, p. 154-
1379 162.
- 1380
- 1381

Figure 1: Physiographic map of the Mediterranean highlighting the main oceanic gateways (in light red) during the Last Glacial Maximum and during the Neogene. The color scale is adapted to the LGM sea level and highlight the main present-day gateways. These gateways control the water, sediment, and biotope exchange between sub-basins and oceans.

1383 **Figure 2:** Illustration of the general palaeoenvironmental and structural framework compiled
 1384 from [Vezzani et al., \(2010\)](#); [Bigi et al., \(1990\)](#); [van Hinsbergen et al., \(2020\)](#). The structural zones
 1385 are associated with the deformation fronts of the Apennines, Dinarids and Albano-Hellenid
 1386 (synthesized from [Zappaterra, 1994](#); [Vezzani et al., 2010](#); [van Hinsbergen et al., 2020](#); this
 1387 study). Sestri-Voltaggio lineament (S.V.); the Anzio-Ancona lineament (A.A.); Maiella-
 1388 Roccamonfina lineament (M.R.); M.A.R. – Mid-Adriatic Ridge; T.R. – Tremiti Ridge; M.F.S. –
 1389 Mattinata Fault System; CAB – Central Adriatic Basin; SAB – South Adriatic Basin.

1390 **Figure 3:** Synthesis of the evolution of the Cenozoic deposit environments specific to each palaeogeographic domain developed during the Mesozoic (synthesized from [Vezzani et al., 2010](#)).
 1391 The involvement of palaeogeographic domain inside the fold-and-thrust belt and the associated
 1392 wedge-top formation are represented in orange. Major tectonic phase reported by [Vezzani et al.](#)
 1393 [\(2010\)](#) are highlighted in light red and numbered from 1 to 6.
 1394

Figure 4:

Previously published MSC formations along the Central Mediterranean area.

Liguri-Provence Basin ([Sage et al., 2005](#); [Lofi et al., 2011](#); [Bache et al., 2015](#)). Tyrrhenian Sea ([Lymer et al., 2018](#)). **Sicily and Calabria** ([Butler et al., 1995, 2019](#) ; [Pedley et al., 2007](#); [El Euch-El Kundi et al., 2009](#); [Roveri et al., 2008a](#); [Henriquet et al., 2020](#) ; [Cavazza and DeCelles, 1998](#)). **Northern and Central Apennine Chain** ([Roveri et al., 2005, 2008b](#); [Ghielmi et al., 2013](#); [Rossi et al., 2015](#); [Pellen et al., 2017](#); [Manzi et al., 2013, 2020](#); [Iaccarino et al., 2008](#); [Milli et al., 2006, 2007](#); [Artoni, 2003](#); [Bigi et al., 2009](#)). **South Apennine Chain** ([Vezzani et al., 2010](#); [Manzi et al., 2020](#)). **South Adriatic Basin** ([Fraseri et al., 2009](#); [Silo et al., 2013](#); [Argnani et al., 2009](#)). **Ionian Basin** ([Micallef et al., 2018](#) ; [Garcia-Castellanos et al., 2020](#) ; [Gutcher et al., 2017](#)).

Table 01: Correlation table of the different deposit units identified along the Apennine fore-deep by [[Milli et al., 2007](#)] compared to the nomenclature of [Roveri et al. \[2004, 2005\]](#).

Legend: pre-ev: pre-evaporitic unit; post-ev: post-evaporitic unit. U1, U2, U3 and I1, I2, I3 are non-conforming surfaces. The dashed line indicates the position of the cinerite level.

Figure 5: Map showing our new interpretation of the sedimentary facies and stratigraphic units observed along the Adriatic Sea and associated with the Messinian event. The mapping of geological formations on land refers to that used in the figure 4. The Messinian-Pliocene basal (yellow to bluish) and Tortonian (pinkish) deposits are highlighted.

Table 02: Stratigraphic chart correlation

Figure 6a: Stratigraphic correlation between 6 boreholes selected on both sides of the promontory of Gargano. This synthesis highlights a different sedimentary filling dynamics in the Tertiary between the CAB (Central Adriatic Basin) and SAB (South Adriatic Basin).

Figure 6b: Illustration of three stratigraphic sections based on industrial boreholes along the CAB and SAB. Significant Oligocene-Tortonian depocenter is observed within the SAB, while strong depocenter is observed during the Pliocene-Quaternary within the CAB.

Figure 7: SW-NE oriented line-drawings along the CAB.

Figure 8: SW-NE oriented line-drawings along the SAB.

Figure 9: Detailed seismic sections (location Figure 8) highlighting the initiation (left) and lateral evolution (right) of the Mass Transport Deposit which mainly compose the M3 seismic unit. The lateral transition from chaotic to continuous seismic reflections allowed to identify the western limit of the MTD observed on Figure 5.

Table 3: Retro-translation and back-rotation values of Adria, Africa, and Calabria-Peloritain blocks with respect to stable Europe (and Corsica-Sardinia blocks). Sources: Sioni (1996); Fidalgo-González (2001), this study.

Figure 10:

A (Top): Palinspastic reconstruction of the Central Mediterranean area at 7.2 Ma.

B (Bottom): Palaeoenvironmental reconstruction of the Central Mediterranean area at 7.2 Ma.

Figure 11:

A (Top): Palinspastic reconstruction of the Central Mediterranean area at 5.9 Ma.

B (Bottom): Palaeoenvironmental reconstruction of the Central Mediterranean area at 5.9 Ma.

Figure 12:

A (Top): Palinspastic reconstruction of the Central Mediterranean area at 5.6 Ma.

B (Bottom): Palaeoenvironmental reconstruction of the Central Mediterranean area at 5.6 Ma.

Figure 13:

A (Top): Palinspastic reconstruction of the Central Mediterranean area at 5.5 Ma.

B (Bottom): Palaeoenvironmental reconstruction of the Central Mediterranean area at 5.5 Ma.

Figure 14:

A (Top): Palinspastic reconstruction of the Central Mediterranean area at 5.36 Ma.

B (Bottom): Palaeoenvironmental reconstruction of the Central Mediterranean area at 5.36 Ma.

Figure 15:

A (Top): Palinspastic reconstruction of the Central Mediterranean area at 5.3 Ma.

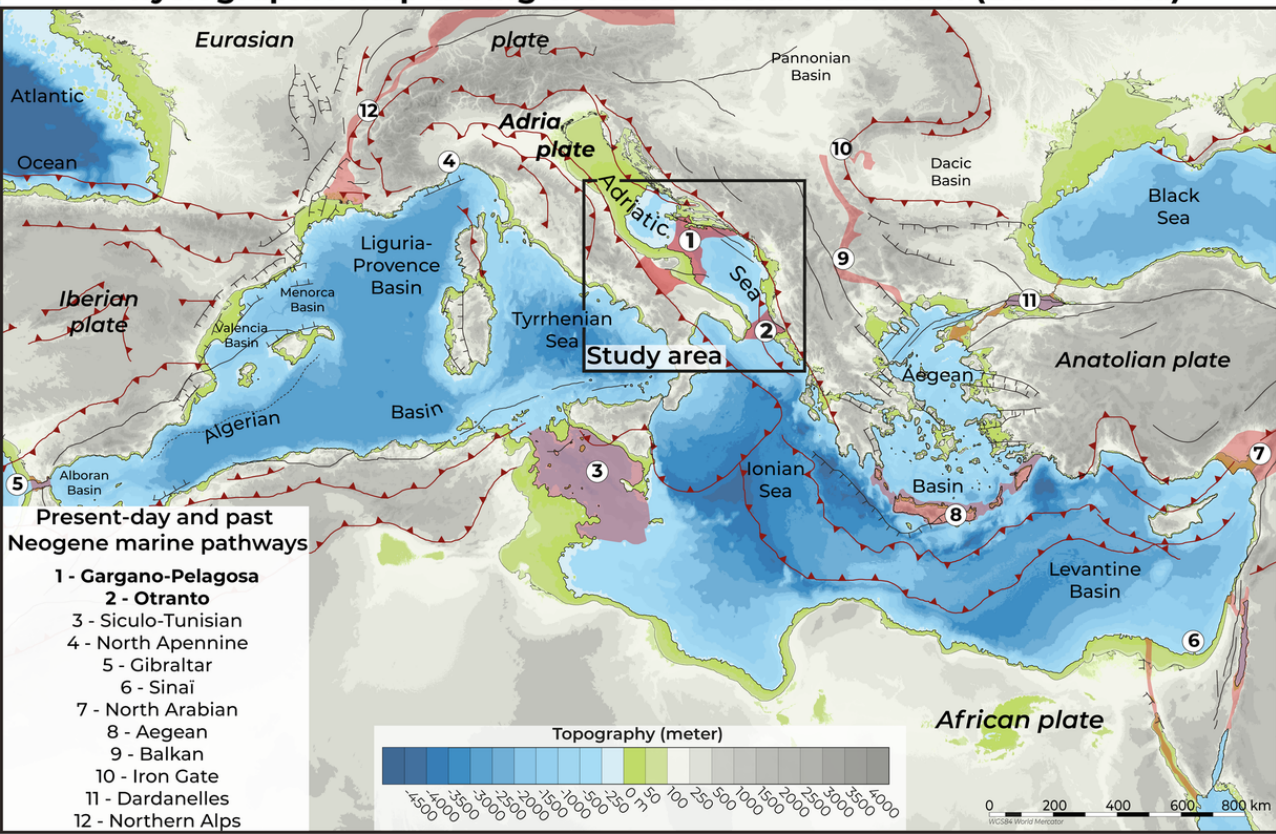
B (Bottom): Palaeoenvironmental reconstruction of the Central Mediterranean area at 5.3 Ma.

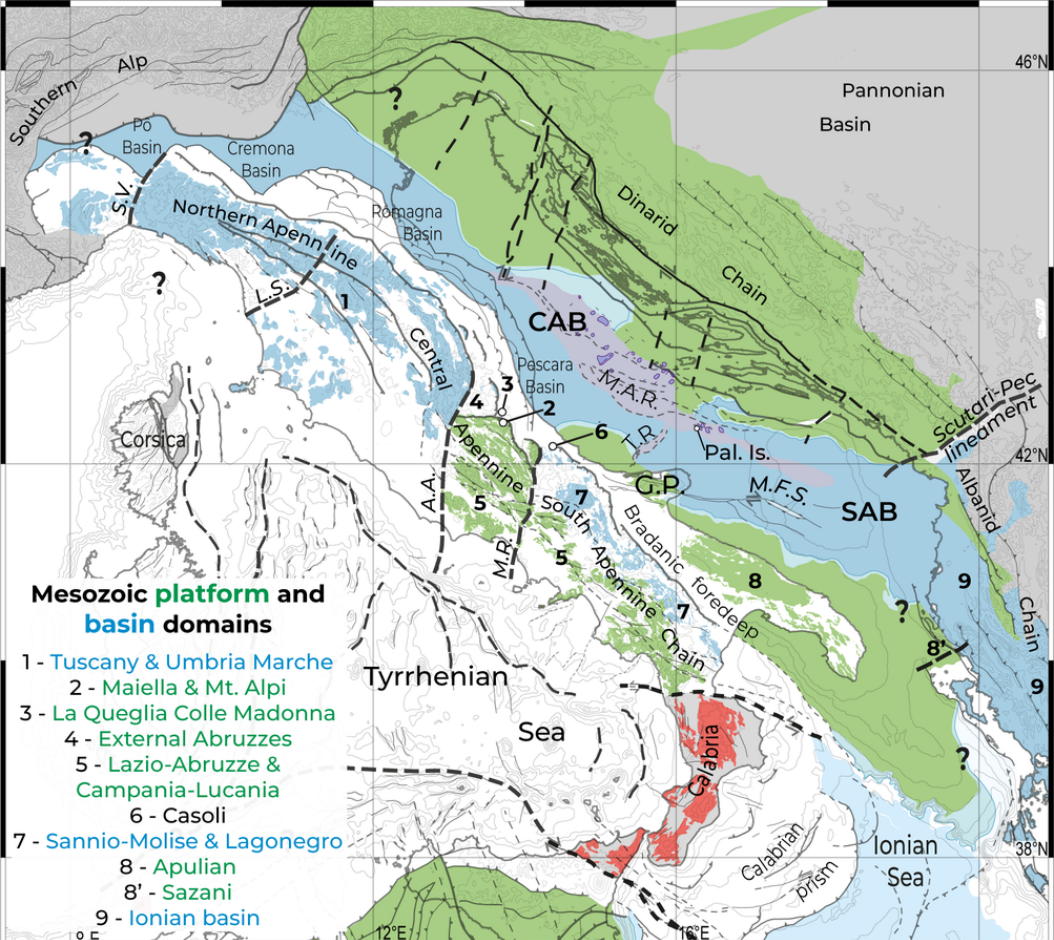
Figure 16:

Monte Ferrara section belonging to the evaporitic Formation of the Castello Mounts, located SE of the Gargano Peninsula (Geographic location Figure 5). The base of the MSC Monte Ferrara succession lies conformably on the Serravallian-Tortonian Serra Palazzo Fm., where primary gypsum facies (massive, banded and branching selenite) are defined.

A major unconformity erodes the Primary Lower Gypsum, then overlapped by pluri-decametric PLG blocks and rich gypso-aneitic beds composing the Resedimented Lower Gypsum. Desiccation cracks and brecciated deposits at the level of the angular unconformity suggest a possible subaerial exposure of the whole Castello Evaporitic Fm. along the south Apennine Chain.

Physiographic map during the Last Glacial Maximum (LGM ~20 ka)



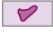





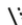




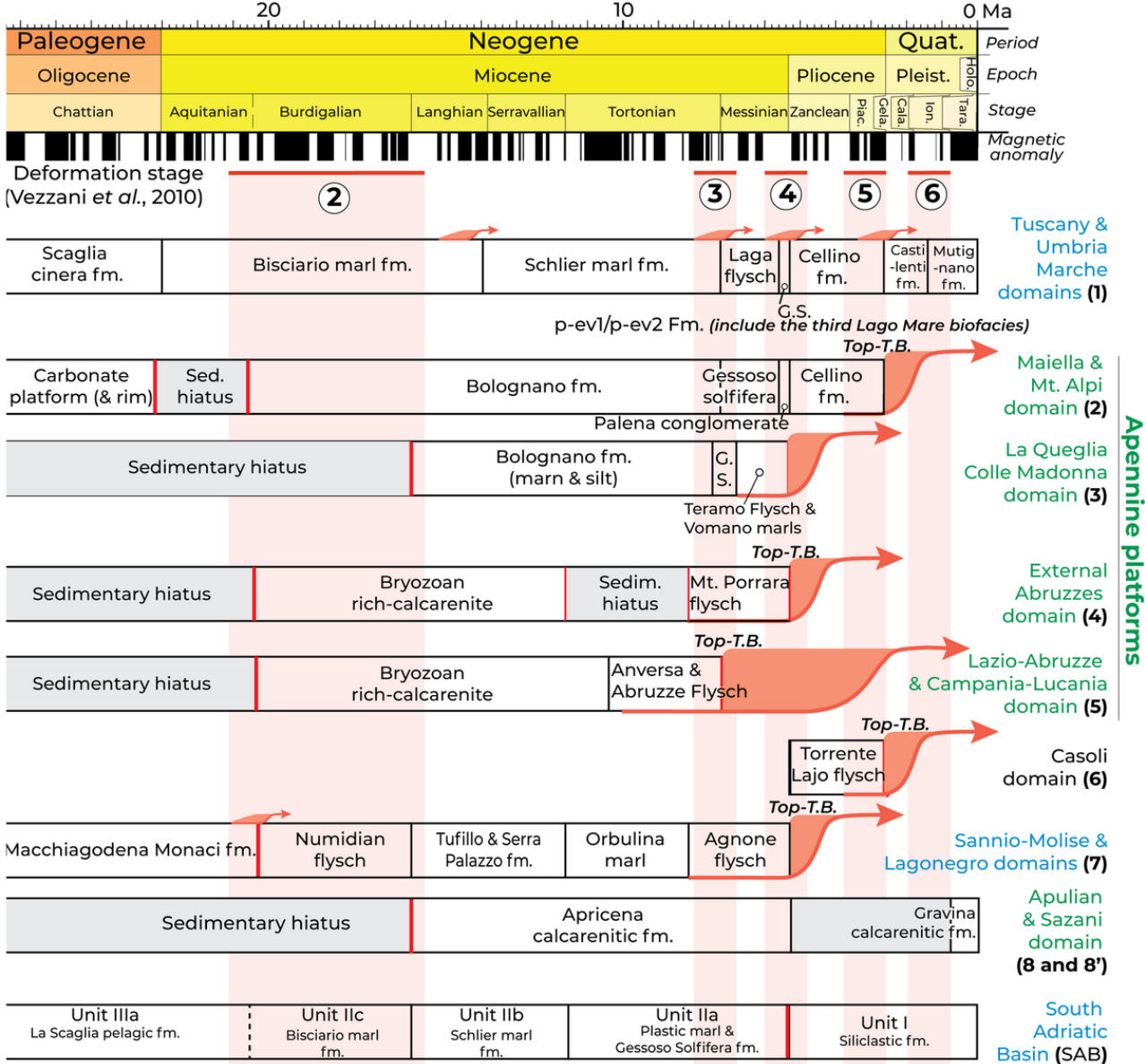
Mesozoic platform and basin domains

- 1 - Tuscany & Umbria Marche
- 2 - Maiella & Mt. Alpi
- 3 - La Queglia Colle Madonna
- 4 - External Abruzzes
- 5 - Lazio-Abruzzes & Campania-Lucania
- 6 - Casoli
- 7 - Sannio-Molise & Lagonegro
- 8 - Apulian
- 8' - Sazani
- 9 - Ionian basin

Physiographic domains and main tectonic features

<p> Mesozoic carbonate platform domain and slope area</p> <p> Mesozoic carbonate basin domain</p>	<p> Estimated zone influenced by the Mid Adriatic Ridge (M.A.R.) and Tremiti Ridge (T.R.)/Triasic salt diapir</p> <p> Ophiolite formations & Mesozoic Terranes</p>	<p>Tectonic feature</p> <p> Normal</p> <p> Transform</p> <p> Thrust</p> <p> Other fault</p> <p> Passive margin hinge line (observed / suspected)</p>
---	--	--

0 100 200 km

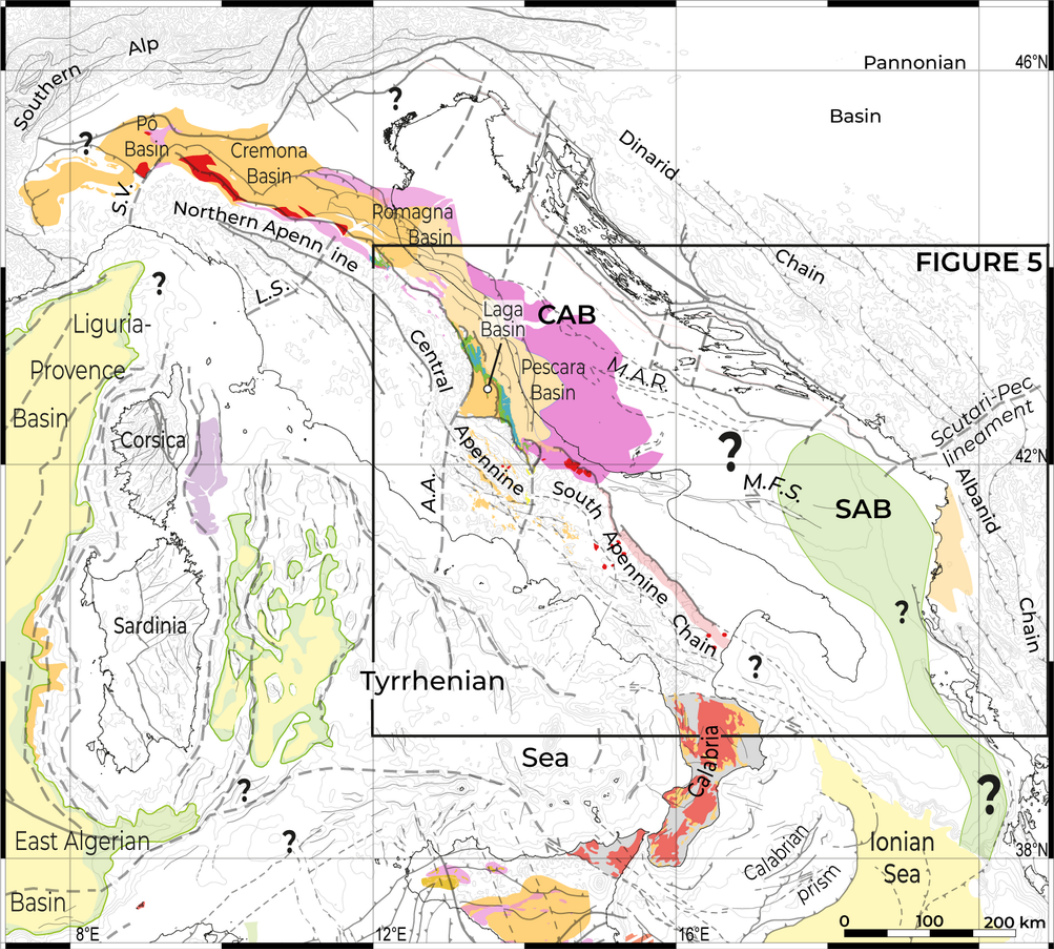


Top-thrust basin formation included in the Apennine FTB (a) and/or domain included in the Apennine FTB (b).




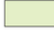


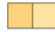



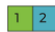


Top-T.B. : Top-Thrust Basin

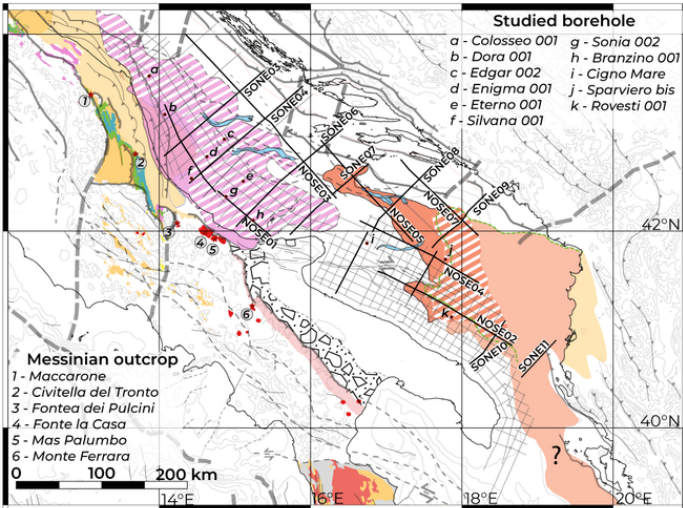
G.S. : Gessoso Solfifera evaporitic formation

p-ev: Post-evaporitic formation

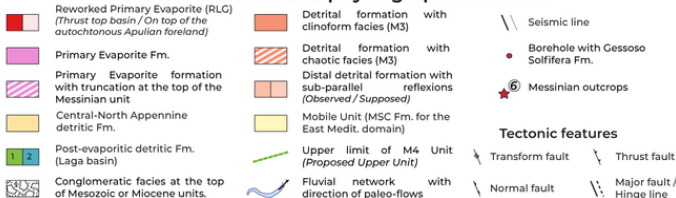


MSC formations and physiographic features

- | | | | |
|---|---|--|---|
|  Reworked Primary Evaporite (RLG) (Thrust top basin / On top of the autochthonous Apulian foreland). |  Detrital fm. with chaotic facies (Mass Transport Deposit - MTD) | Tectonic feature | |
|  Primary Evaporite Fm. |  Upper Unit |  Normal |  Transform |
|  Detrital Fm. (including RLG along Apennine foredeep) (Observed / Supposed) |  Bedded Unit |  Thrust |  Other fault |
|  Post-evaporitic Fm. (Laga basin) |  Mobile Unit (MSC Fm. for the East Medit. domain) |  Passive margin hinge line (observed / suspected) | |



MSC formations and physiographic features



● Colosseo 001

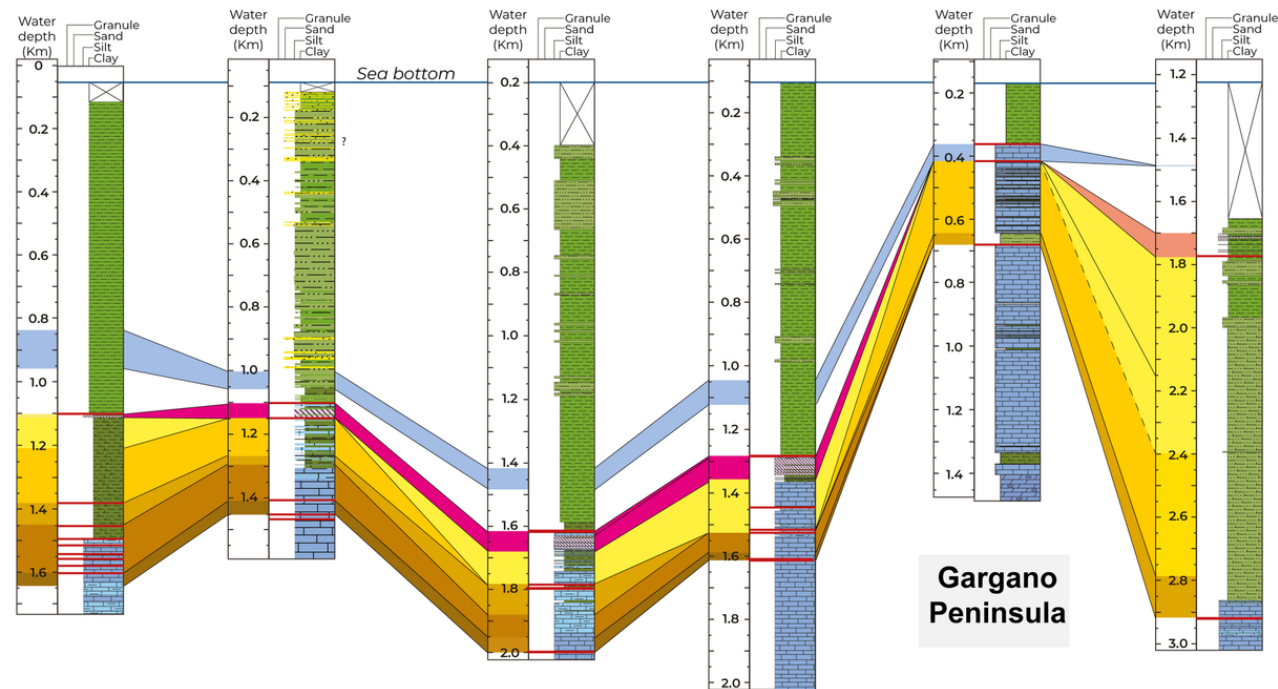
● Dora 002

● Enigma

● Branzino

● Cigno Mare

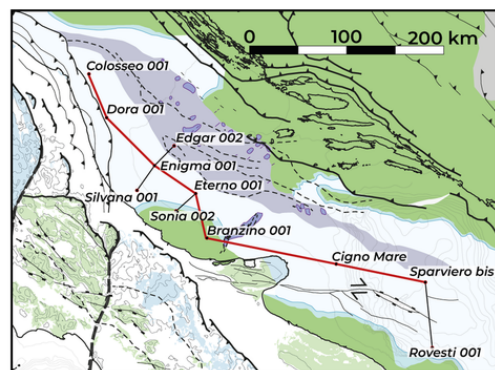
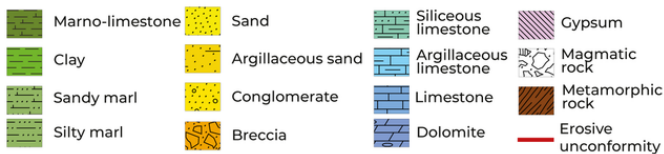
● Sparviero bis

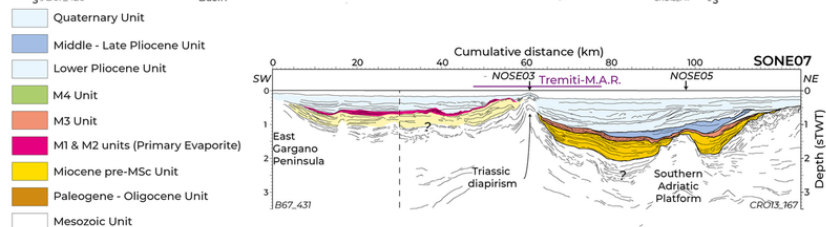
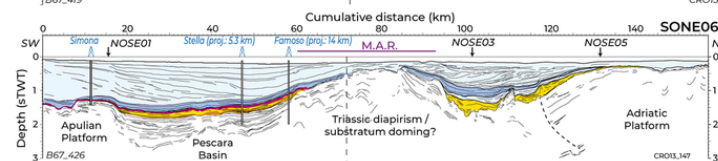
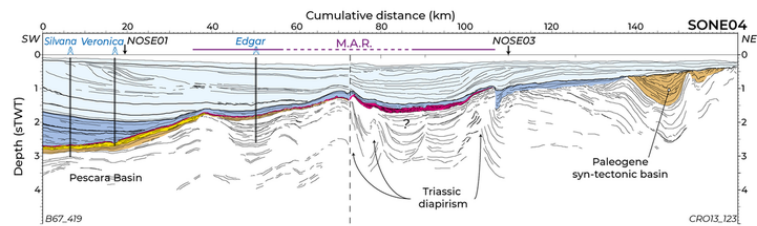
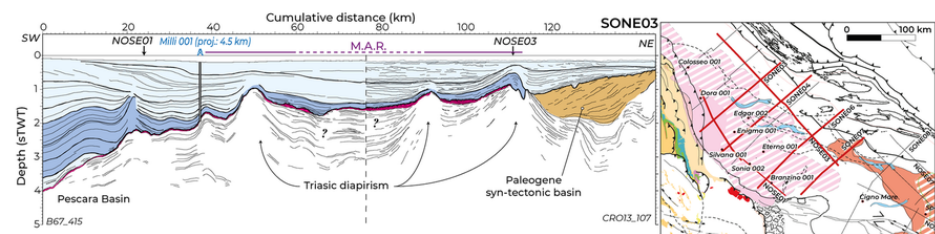
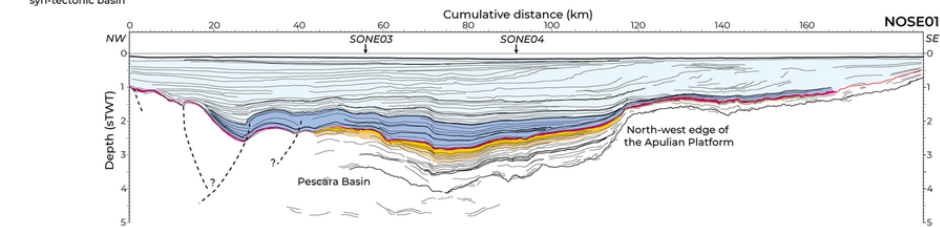
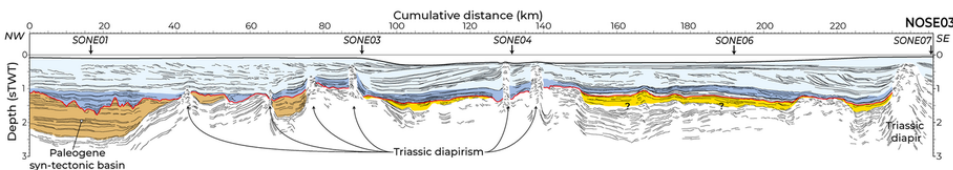


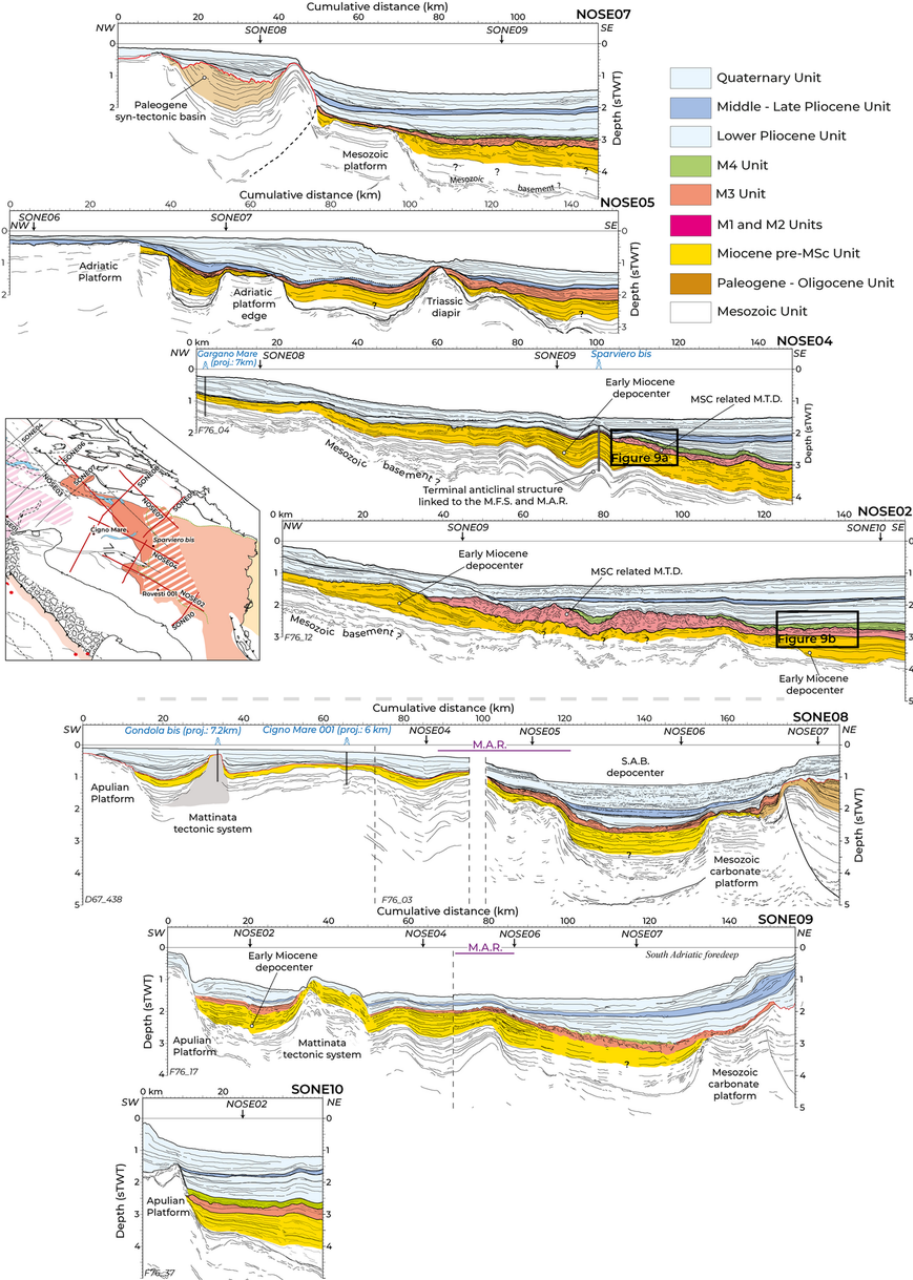
Geological age

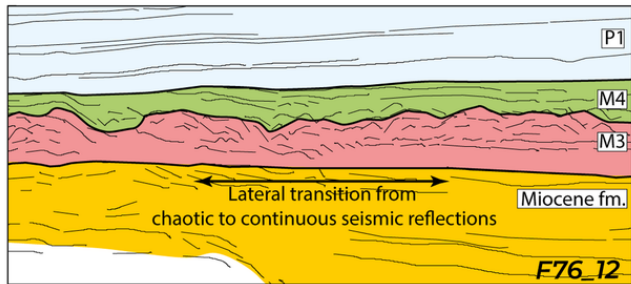
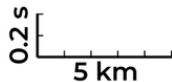
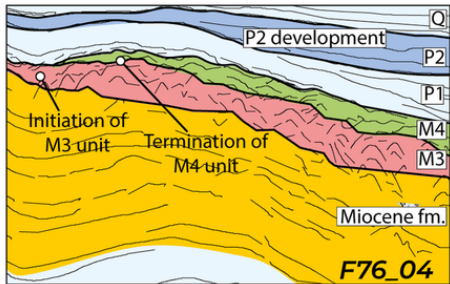
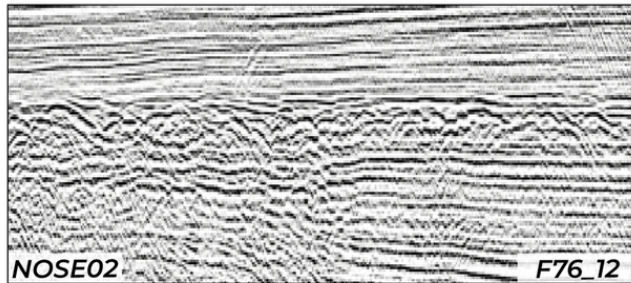
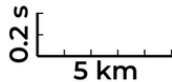
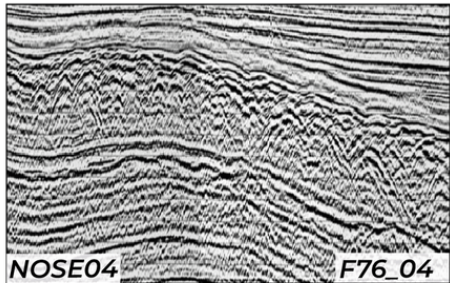


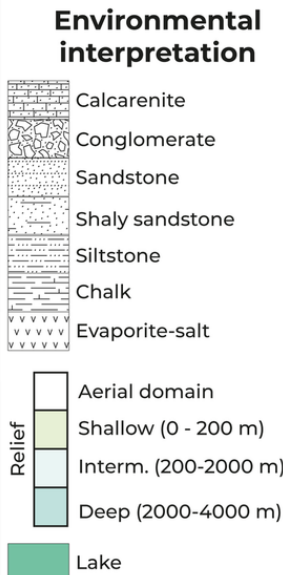
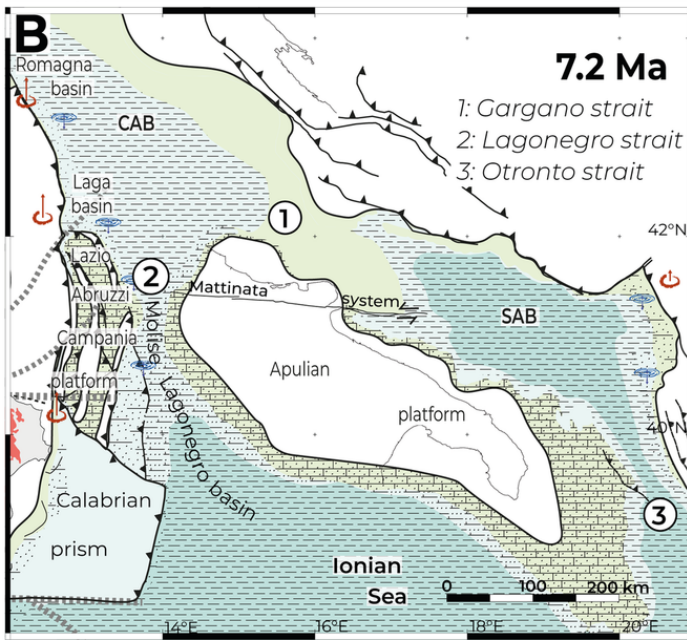
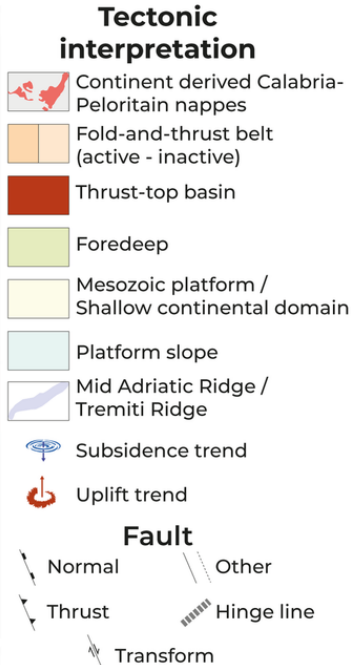
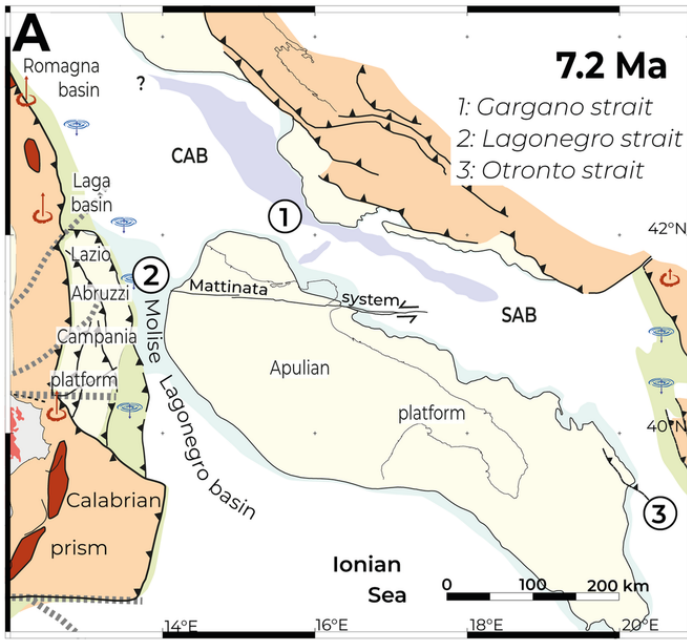
Lithologic facies

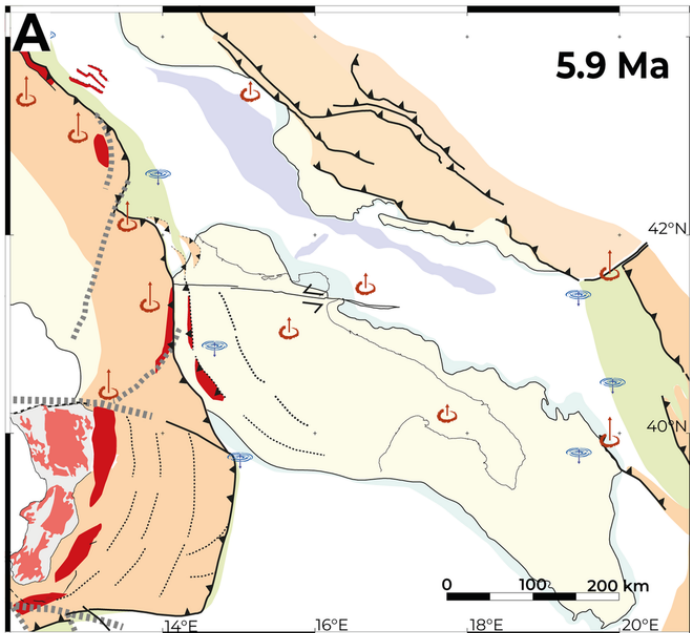





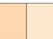














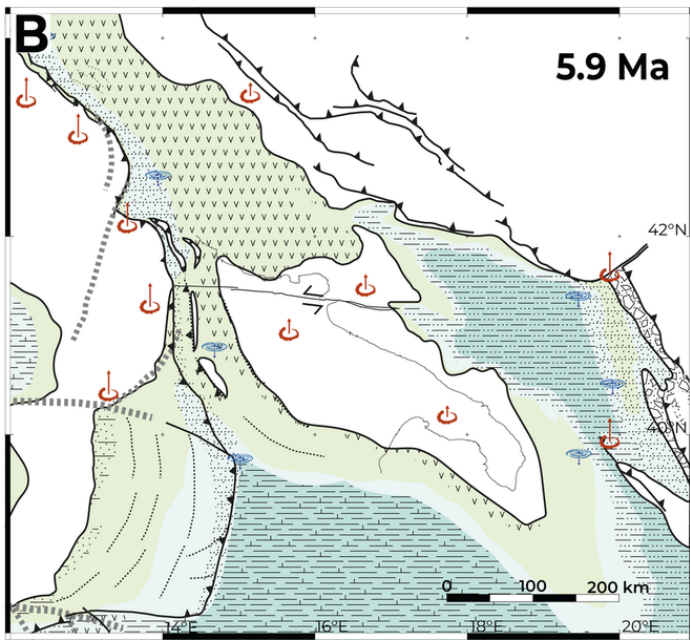












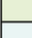





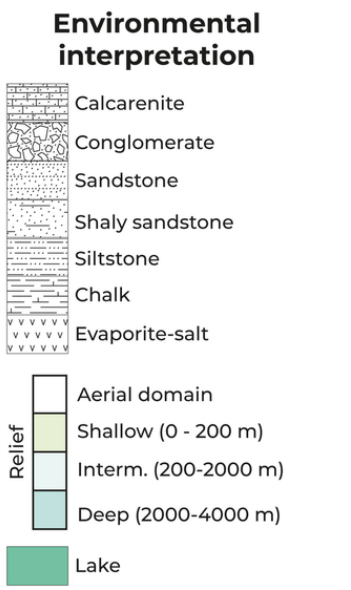
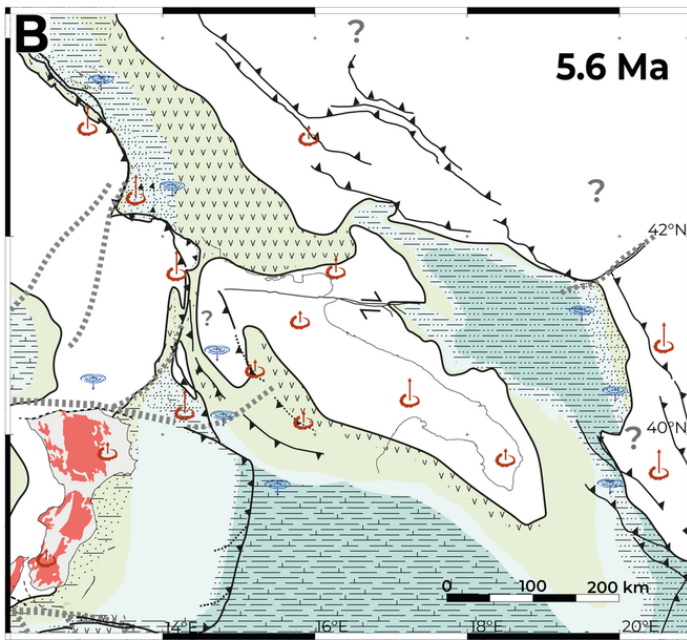
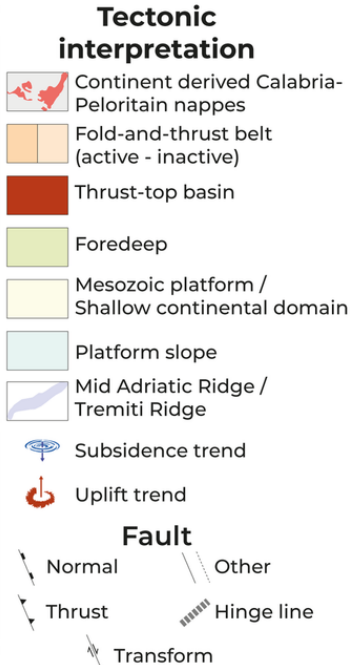
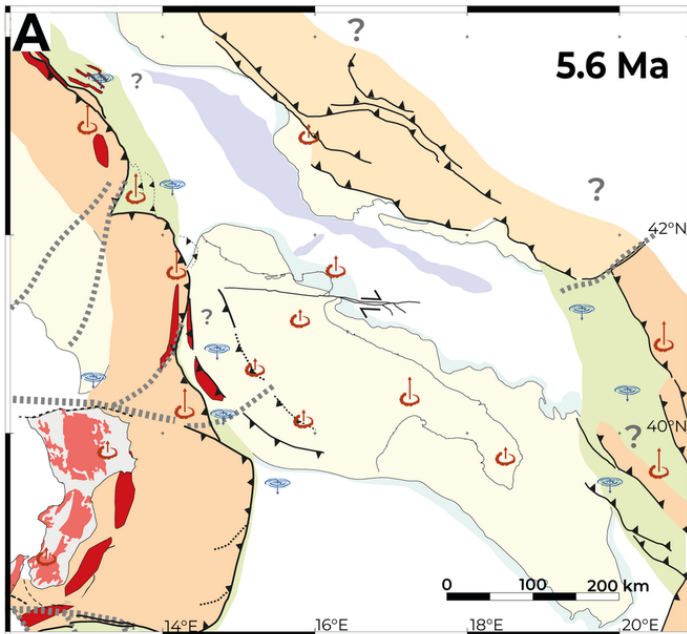
Tectonic interpretation

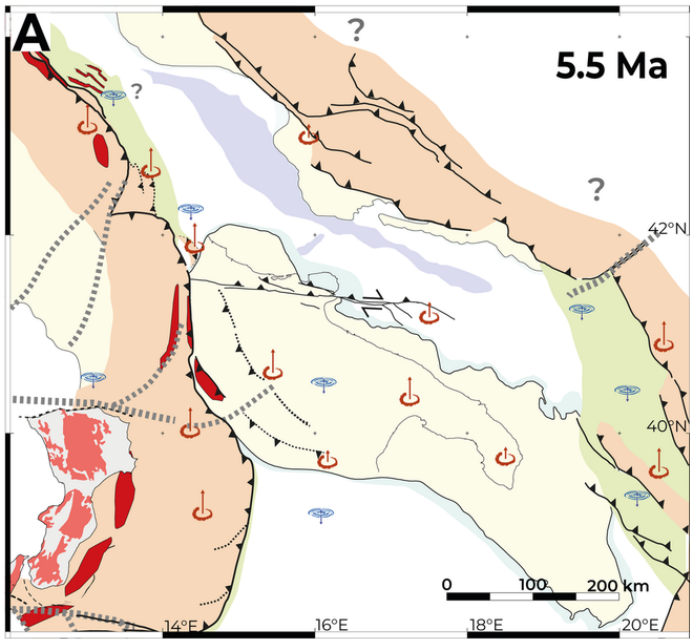
-  Continent derived Calabria-Peloritain nappes
 -  Fold-and-thrust belt (active - inactive)
 -  Thrust-top basin
 -  Foredeep
 -  Mesozoic platform / Shallow continental domain
 -  Platform slope
 -  Mid Adriatic Ridge / Tremiti Ridge
 -  Subsidence trend
 -  Uplift trend
- ### Fault
-  Normal
 -  Thrust
 -  Transform
 -  Other
 -  Hinge line



Environmental interpretation

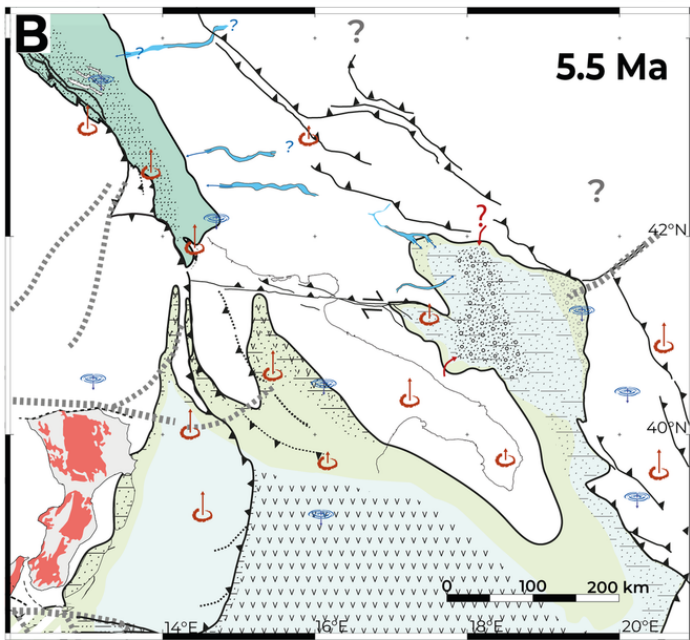
-  Calcarenite
 -  Conglomerate
 -  Sandstone
 -  Shaly sandstone
 -  Siltstone
 -  Chalk
 -  Evaporite-salt
- ### Relief
-  Aerial domain
 -  Shallow (0 - 200 m)
 -  Interm. (200-2000 m)
 -  Deep (2000-4000 m)
 -  Lake





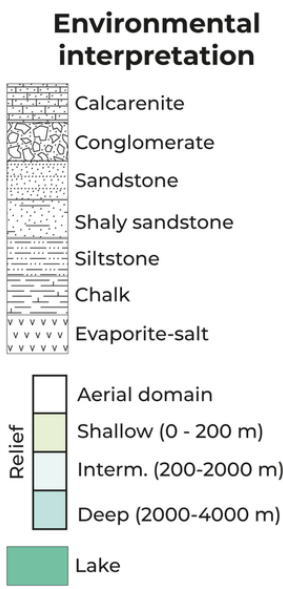
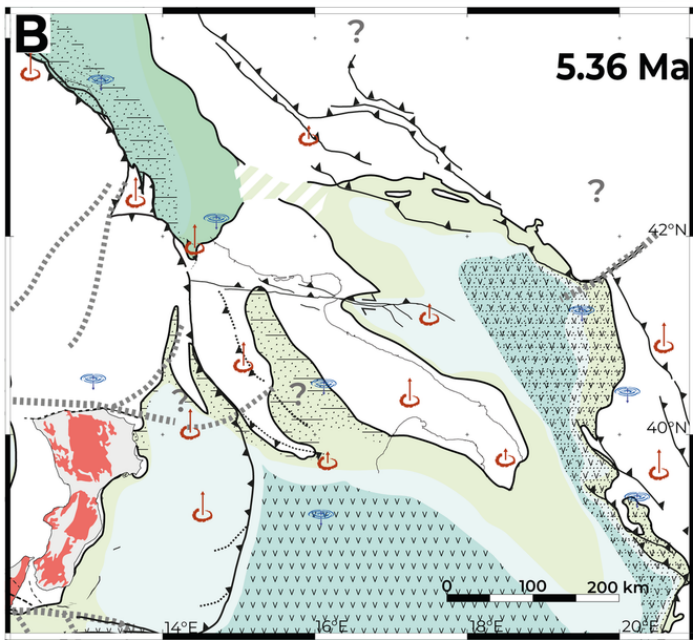
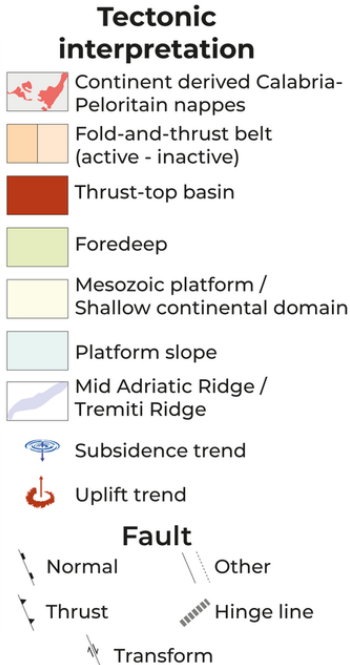
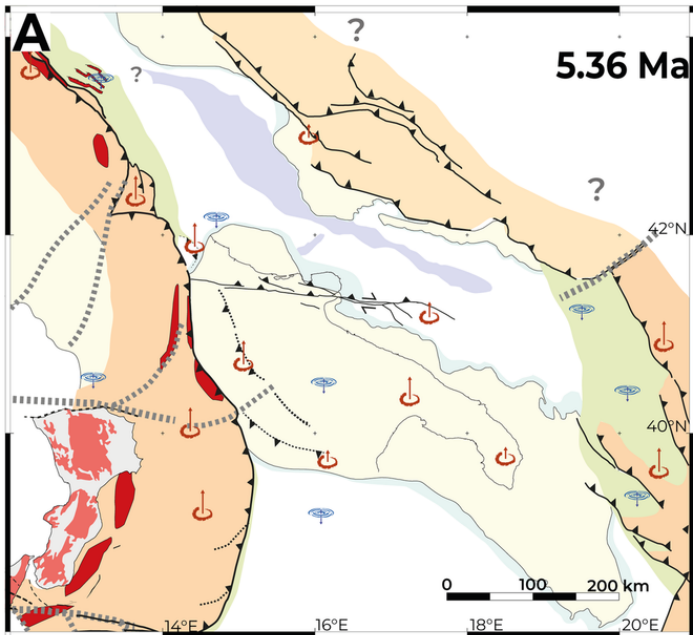
Tectonic interpretation

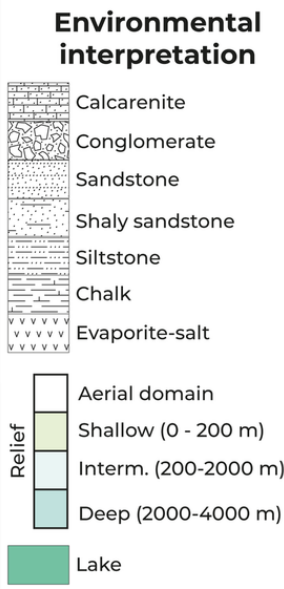
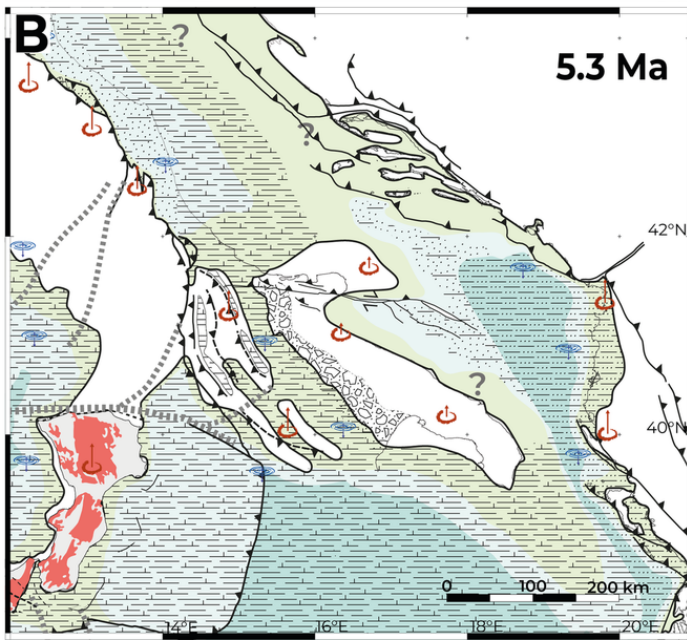
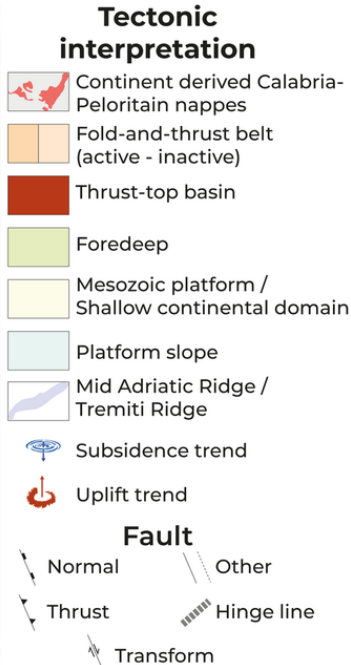
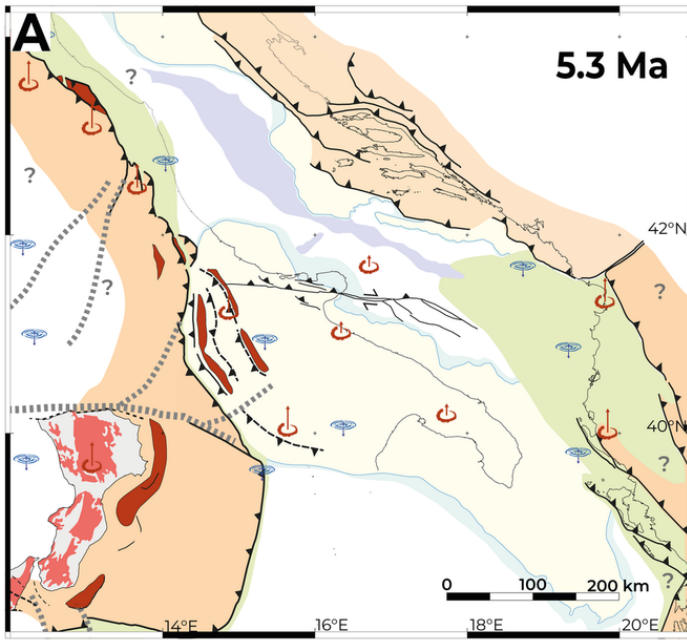
- Continent derived Calabria-Peloritain nappes
 - Fold-and-thrust belt (active - inactive)
 - Thrust-top basin
 - Foredeep
 - Mesozoic platform / Shallow continental domain
 - Platform slope
 - Mid Adriatic Ridge / Tremiti Ridge
 - Subsidence trend
 - Uplift trend
- ### Fault
- Normal
 - Thrust
 - Other
 - Hinge line
 - Transform



Environmental interpretation

- Calcarenites
 - Conglomerate
 - Sandstone
 - Shaly sandstone
 - Siltstone
 - Chalk
 - Evaporite-salt
- ### Relief
- Aerial domain
 - Shallow (0 - 200 m)
 - Interm. (200-2000 m)
 - Deep (2000-4000 m)
- Lake
 - Incised-valley system



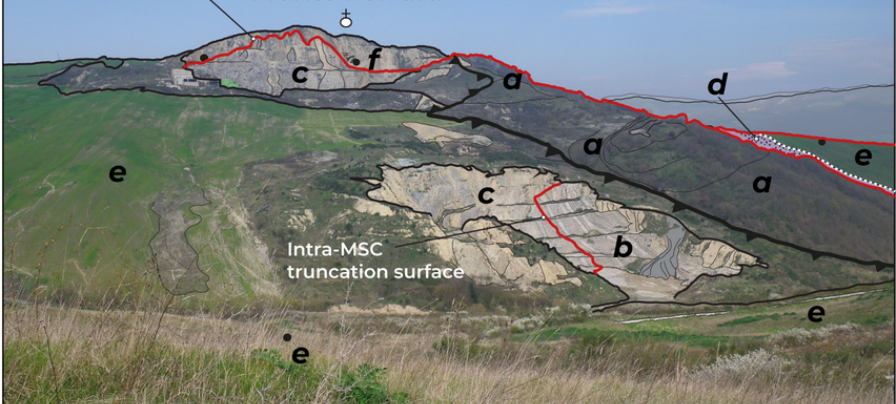


SSW

NNE

Top Messinian-Pliocene
truncation surface

Monte Ferrara

**Serravallian - Tortonian**

- a** Serra Palazzo fm.
(Serravallian - Tortonian)

Messinian syn-MSC

- b** Ribboned gypsum beds
(Primary Lower Gypsum)
- c** Reworked evaporite gypsum
with PLG microblocks.

Zanclean-Piacenzian

- d** Conglomerate to
calc-arenite formation
- e** Blue clay formation

Lower Pleistocene

- f** Stratified silt-argilleous
formation

 Erosive
unconformity

 Thrust

 Biostratigraphic
sample

Central Apennine stratigraphy

Pô plain		Romagna Basin			Laga Basin						
Ghielmi et al., 2010		Roveri et al., 2004, 2005			Artoni, 1993	Artoni, 2003	Milli et al., 2007		Centamore and Nisio, 2003		
	Marginal basins	Deep basins	Sequence		allounits	allounits	allounits	sequence	sequence	Lithostratigraphic units	
PL ₁	Argile Azzurre	Argile Azzurre	U.B.S.U.		Unit 0	Pliocene			P1a	P1	
M ₄	Colombacci fm.	Colombacci fm.	p-ev2	MP	Colombacci unit	p-ev2	Laga 3	Cellino depositional sequence	M3b	Post-evaporitic member	
LM	hiatus	S. Donato fm.	p-ev1		post-ev pelitic unit	U4			M3a		
M ₃	intra-messinian unconformity	ash layer Sapigno fm.			post-ev arenaceous fm.	post-ev arenaceous fm.			M2b		
M ₂	Vena del Gesso fm. (ex. Gessoso Solfifera fm. shallow water member) Autochthonous evaporite	'euxinic shales'			Evaporitic member	ev	Laga 2	Laga depositional sequence	M2a	M2	Evaporitic member
M ₁	Marnoso-arenacea fm. 'euxinic shales'				Pre-evaporitic member	pre-ev	Laga 1		M1	M1	Pre-evaporitic member
T ₂				T ₂		U1	l1	Marnoso depo. seq.			Cerrogna marls and Pteropoda
						Cerrogna marls	Cerrogna marls	Cerrogna marls			

5.33 Ma

5.42 Ma

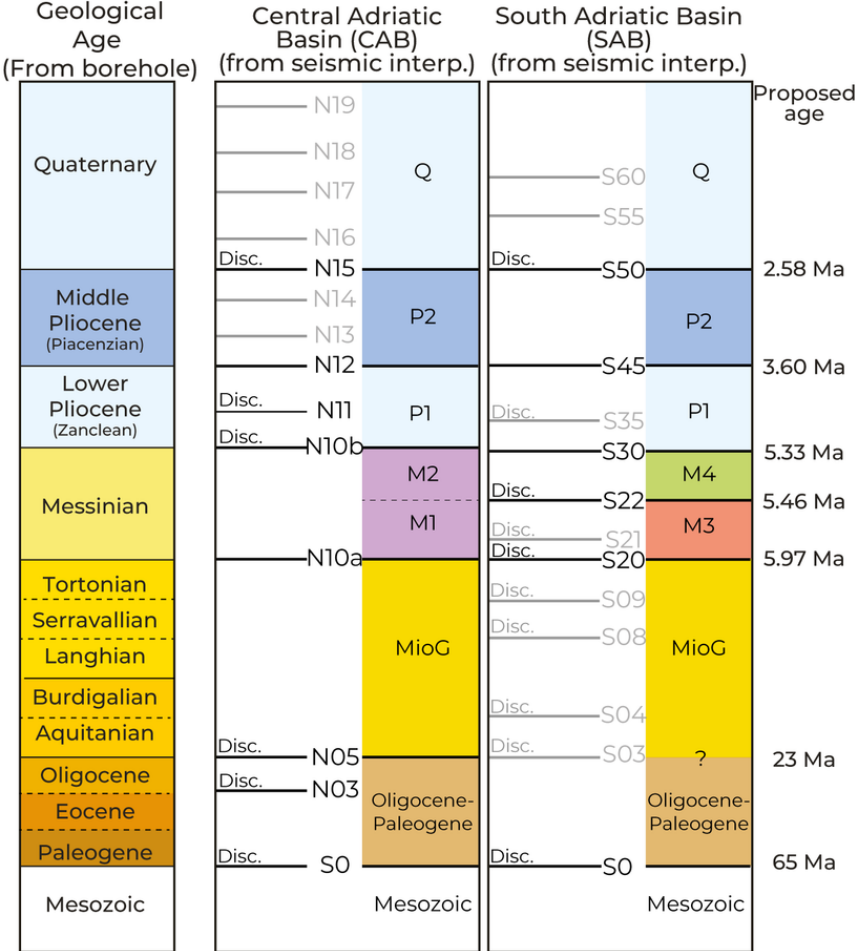
5.6 Ma

5.97 Ma

7.25 Ma

Cellino depositional sequence

Laga depositional sequence



Disc. Discontinuity discussed in this study

Disc. Other discontinuity observed by seismic observation

Magnetic anomaly / Aged step	Geological age (Ma)	Rotation parameters		
		Latitude	Longitude	Angle

Motion of Adria vs Eurasian plate (Sioni, 1996)

Ano0	0.0	0	0	0
Ano6	20.0	42.8	5.1	-5.7

Motion of Calabria vs Eurasian plate (this study)

Ano0	0.0	0	0	0
Age2.5	2.5	-14.9	-168.9	-3.0
Age4	4.0	-14.3	-170.5	-4.8
Age7.2	7.2	-14.3	-170.5	-8.7
Ano6	20.0	47.0	12.9	-47.8

Motion of Africa-Sicily vs Eurasian plate (Fidalgo, 2001)

Ano0	0.0	0	0	0
Ano5	8.92	15.2	-20.4	-0.9
Ano6	20.0	15.0	-18.6	-2.1